# Leaf Wax Hydrogen Isotopes as a Hydroclimate Proxy in the Tropical Pacific

Sarah Nemiah Ladd[1,1,1], Ashley Elizabeth Maloney[2,2,2], Daniel Nelson[3,3,3], Matthew Prebble[4,4,4], Giorgia Camperio[1,1,1], David Ayres Sear[5,5,5], Jonathan Hassall[5,5,5], Peter Langdon[5,5,5], Julian P Sachs[6,6,6], and Nathalie Dubois[1,1,1]

[1]Eawag
[2]Princeton University
[3]University of Basel
[4]University of Canterbury
[5]University of Southampton
[6]University of Washington

November 30, 2022



## Abstract

The hydrogen isotope composition ($^{2}H/^{1}H$ ratios) of leaf waxes preserved in sediments is increasingly used to reconstruct past hydroclimate. Here, we extend the global calibration of leaf wax $^{2}H/^{1}H$ ratios to include surface sediments from 23 lakes and swamps on 15 tropical Pacific islands. Leaf wax $^{2}H/^{1}H$ ratios from this new data set are not correlated with regional estimates of mean annual precipitation $^{2}H/^{1}H$ ratios derived from isoscapes or from isotope-enabled general circulation models. Nevertheless, the new data fall within the predicted range of values based on a global calibration compiled from published surface sediments. In our global compilation, we find a strong positive linear correlation between $^{2}H/^{1}H$ ratios of mean annual precipitation and the common leaf waxes n-C29-alkane ($R^{2}$ = 0.73, n = 581) and n-C28-acid ($R^{2}$ = 0.74, n = 242). In the tropical Pacific, the largest residuals are no greater than those observed elsewhere, and are likely due to (1) uncertainty in the $^{2}H/^{1}H$ ratios of local precipitation and (2) variability in net fractionation for different plant types. Palynological analyses from the same samples suggest that there is no systematic relationship between any particular type of pollen distribution and deviations from the global calibration line. Overall, our results support the use of leaf wax $^{2}H/^{1}H$ ratios in tropical Pacific lake sediments as proxies for large hydrological changes, especially when paired with $^{2}H/^{1}H$ ratios of source-specific biomarkers. However, the interpretation of such records needs to be informed by careful consideration of local drivers of precipitation isotope variability.

## Hosted file

`ladd_et_al_supporting-information.docx` available at https://authorea.com/users/558429/articles/607629-leaf-wax-hydrogen-isotopes-as-a-hydroclimate-proxy-in-the-tropical-pacific

# Leaf Wax Hydrogen Isotopes as a Hydroclimate Proxy in the Tropical Pacific

**S. N. Ladd[1,2*], A. E. Maloney[3,4], D. B. Nelson[5], M. Prebble[6,7], G. Camperio[1,2], D. A. Sear[8], J. D. Hassall[8], P. G. Langdon[8], J. P. Sachs[3], and N. Dubois[1,2]**

[1]Swiss Federal Institute of Aquatic Science and Technology (EAWAG), Dept. of Surface Waters – Research and Management, Dübendorf, CH. [2]Swiss Federal Institute of Technology (ETH-Zürich), Dept. of Earth Sciences, Zürich, CH. [3]University of Washington, School of Oceanography, Seattle, USA. [4]Princeton University, Dept. of Geosciences, Princeton, USA. [5]University of Basel, Dept. of Environmental Sciences-Botany, Basel, CH. [6]University of Canterbury, School of Earth and Environment, Christchurch, NZ. [7]Australian National University, School of Culture, History and Languages, Canberra, AU. [8]University of Southampton, School of Geography and Environmental Science, Southampton, UK.

Corresponding author: S. Nemiah Ladd (nemiah.ladd@cep.uni-freiburg.de)

*Current address: University of Freiburg, Ecosystem Physiology, Freiburg, DE

**Key Points:**

- Leaf wax $^{2}H/^{1}H$ ratios are correlated with mean annual precipitation $^{2}H/^{1}H$ ratios globally, but not in the tropical Pacific
- Deviations from the global relationship between precipitation leaf wax $^{2}H/^{1}H$ ratios cannot be predicted from palynological assemblages
- Small range and large uncertainties in estimates of tropical Pacific precipitation $^{2}H/^{1}H$ ratios likely account for poor correlations

## Abstract

Hydrogen isotope ratios of sedimentary leaf waxes ($\delta^2H_{Wax}$ values) are increasingly used to reconstruct past hydroclimate. Here, we add $\delta^2H_{Wax}$ values from 19 lakes and four swamps on 15 tropical Pacific islands to an updated global compilation of published data from surface sediments and soils. Globally, there is a strong positive linear correlation between $\delta^2H$ values of mean annual precipitation ($\delta^2H_P$ values) and the leaf waxes *n*-$C_{29}$-alkane ($R^2 = 0.74$, n = 665) and *n*-$C_{28}$-acid ($R^2 = 0.74$, n = 242). Tropical Pacific $\delta^2H_{Wax}$ values fall within the predicted range of values based on the global calibration, and the largest residuals from the global regression line are no greater than those observed elsewhere, despite large uncertainties in $\delta^2H_P$ values at some Pacific sites. However, tropical Pacific $\delta^2H_{Wax}$ values in isolation are not correlated with estimated $\delta^2H_P$ values from isoscapes or from isotope-enabled general circulation models. Palynological analyses from these same Pacific sediment samples suggest no systematic relationship between any particular type of pollen distribution and deviations from the global calibration line. Rather, the poor correlations observed in the tropical Pacific are likely a function of the small range of $\delta^2H_P$ values relative to the typical residuals around the global calibration line. Our results suggest that $\delta^2H_{Wax}$ values are currently most suitable for use in detecting large changes in precipitation in the tropical Pacific and elsewhere, but that ample room for improving this threshold exits in both improved understanding of $\delta^2H$ variability in plants, as well as in precipitation.


## Plain Language Summary

Past precipitation patterns are difficult to reconstruct, limiting our ability to understand Earth's climate system. Geochemists reconstruct past precipitation by measuring the amount of

heavy hydrogen naturally incorporated into the waxy coating of leaves, which is preserved in mud that accumulates in lakes, soils, and oceans. Heavy hydrogen in leaf waxes is strongly correlated with local precipitation, allowing us to learn about rainfall intensity, temperature, and cloud movement. However, no existing calibration studies include sites from the tropical Pacific, home to the most intense rainfall on the planet and populations that rely on rain for drinking water. We measured heavy hydrogen in leaf waxes from tropical Pacific islands and show that although values are within the global calibration error, no precipitation relationship exists within the region. Plant type distributions do not explain the lack of correlation, which is best attributed to poorly constrained estimates of heavy hydrogen in local rain and the relatively small range of variability within the region. At present, heavy hydrogen from ancient leaf waxes can show large changes in past precipitation, but improved process-level understanding is needed to use this tool to understand smaller changes in the tropical Pacific and elsewhere.

## 1 Introduction

As Earth warms, precipitation intensity, frequency, and spatial distribution are expected to change over the tropical Pacific (Brown et al., 2011; Tan et al., 2015; Sharmila et al., 2018). These predictions need to be constrained and validated by robust reconstructions of past changes, which are unfortunately limited in this region, in part because of a lack of proxies and archives suitable for producing high resolution, continuous records (Hassall 2017). Existing high-resolution paleohydrologic records have been established from speleothems (Partin et al., 2013; Maupin et al., 2014) and corals (Quinn et al., 1993; Quinn et al., 1998; Hendy et al, 2002; Linsley et al., 2004; Linsley et al., 2006; Calvo et al., 2007; DeLong et al., 2012), but are generally limited to the past 600 years in this region. Lacustrine and swamp sediments can provide longer records with much higher temporal resolution than is possible from slowly

accumulating marine sediments, and are well-established archives of ecological, anthropogenic, and broad climatic changes in the region (Southern, 1986; Hope & Pask, 1998; Stevenson et al., 2001; Prebble & Wilmshurst, 2009; Prebble et al., 2019; Gosling et al., 2020). More recently, such sediments have also been used to reconstruct past hydroclimate change in the western tropical Pacific at higher temporal resolution (Sachs et al., 2009; Smittenburg et al., 2011; Konecky et al., 2016; Richey & Sachs, 2016; Hassall, 2017; Sachs et al., 2018; Sear et al., 2020).

One hydroclimate proxy suitable for tropical lake and swamp sediments in the tropical Pacific is based on the hydrogen isotopic composition of leaf waxes ($\delta^2H_{Wax}$= $(^2H/^1H)_{Wax}/(^2H/^1H)_{VSMOW} - 1$) (Sachse et al., 2012; Konecky et al., 2016; Hassall, 2017). $\delta^2H_{Wax}$ values are highly correlated with hydrogen isotopes of mean annual precipitation ($\delta^2H_P$) on a global scale and have been applied to reconstruct $\delta^2H_P$ values in diverse locations (Sachse et al., 2012; McFarlin et al., 2019). $\delta^2H_P$ values are related to specific physical processes, and are a chemical signal that can both be transferred to material preserved on geologic timescales, as well as modeled in modern systems with increasing accuracy, making their reconstructions useful for understanding past hydroclimate dynamics (Bowen et al., 2019).

As is typical for organic geochemical proxies, the relationship between $\delta^2H_{Wax}$ and $\delta^2H_P$ has been established through empirical calibrations with surface sediments from lakes and surface soils. These calibration efforts began in Europe (e.g., Sachse et al., 2004; Leider et al., 2013; Nelson et al., 2018) and have been extended to the Americas (e.g., Hou et al., 2008; Polissar & Freeman, 2010; Douglas et al., 2013), East Asia and the Tibetan Plateau (e.g., Jia et al., 2008; Aichner et al., 2010; Bai et al., 2011), and Africa (e.g., Peterse et al., 2009; Garcin et al., 2012; Schwab et al, 2015) (Figure 1). Recent compilations of $\delta^2H_{Wax}$ from surface sediments (McFarlin et al., 2019) and from sediments and soils (Liu & An, 2019) placed these local

calibrations in a global context. However, existing global compilations do not include any tropical Pacific $\delta^2H_{Wax}$ values.

Two considerations make it important to include tropical Pacific data in the global calibration. Firstly, different vegetation types can influence net community $^2H/^1H$ fractionation between precipitation and leaf waxes, which is not constant among plant types or environments (Feakins and Sessions, 2010; Sachse et al., 2012; Kahmen et al., 2013). The unique plant communities on tropical Pacific islands include many endemic species (Gillespie et al., 2013). Additionally, coastal regions or former lagoons on these islands are often covered by mangrove swamps, which consist of trees and shrubs adapted to brackish to hypersaline water. Due to salinity effects, mangrove $\delta^2H_{Wax}$ values may have the opposite response to changes in precipitation intensity as nearby freshwater plants (Ladd & Sachs, 2012; He et al., 2017). However, the impact of mangrove contributions to sedimentary $\delta^2H_{Wax}$ values has not been assessed.

Secondly, there is large uncertainty associated with estimates of $\delta^2H_P$ in the tropical Pacific. Direct measurements of $\delta^2H_P$ from the Global Network of Isotopes in Precipitation (GNIP) are spatially and temporally limited compared to other regions, resulting in large uncertainties for statistical interpolations of $\delta^2H_P$ such as those used for isoscape products and the Online Isotopes in Precipitation Calculator (OIPC; Bowen & Revenaugh, 2003). Estimates of $\delta^2H_P$ from general circulation models (GCMs) in which precipitation isotopes have been incorporated offer another potential calibration target for $\delta^2H_{Wax}$ measurements in the modern tropical Pacific that has not yet been explored.

Here we measured $\delta^2H$ values of seven *n*-alkane and five *n*-alkanoic acid homologues from surface sediments collected from lakes influenced by precipitation from the South Pacific Convergence Zone (SPCZ) and from mangrove swamps influenced by the Intertropical

Convergence Zone (ITCZ). We add new surface sediment $\delta^2H_{Wax}$ measurements of two of these compounds (*n*-$C_{29}$-alkane and *n*-$C_{28}$-acid) from 19 lakes and four mangrove swamps on 15 islands distributed throughout the tropical Pacific to an updated global compilation of $\delta^2H_{Wax}$ values. We assess whether $\delta^2H_{Wax}$ values from tropical Pacific lake and swamp sediments are consistent with the global relationship between $\delta^2H_{Wax}$ and modeled $\delta^2H_P$ values from a diverse set of algorithms and models. Finally, we use pollen-based vegetation reconstructions to evaluate the influence of plant communities on tropical Pacific $\delta^2H_{Wax}$ values.

## 2 Materials and Methods

### 2.1 Site description and sample collection

Surface sediments were collected from 19 lakes on 11 islands across the SPCZ region (Figure 1, Table 1), ranging in elevation above mean sea level from 790 m (Lanoto'o, Samoa) to 1 m (Rimatu'u, Oroatera, and Onetahi ponds on Tetiaroa, French Polynesia). Lakes ranged from shallow ephemeral water bodies to an 88 m-deep volcanic crater lake (Lake Lalolalo, Wallis). Most lakes were freshwater systems, except for the brackish (salinity = 17) coastal Lake Dranoniveilomo (Fiji) and Lake Lalolalo (Wallis), which has a freshwater surface lens above saline water (Sichrowsky et al., 2014). Mangrove trees surrounded Lake Dranoniveilomo, while many other sites were located in forested regions, some impacted by human activity, particularly horticulture. Aquatic vegetation covered the surface of some lakes (Table 1). Additional samples were obtained from mangrove swamps located within the ITCZ throughout the Federated States of Micronesia and Guam. All swamps were located at sea level and submerged at high tide. Four or five surface sediment samples were collected from each swamp along a transect from the inland edge to the coast.

Maloney et al. (2019) described the collection of most lake samples from the SPCZ region. New samples include those from Lake Dranoniveilomo, which was cored in 2010 with a Universal Percussion Corer (Aquatic Research, Hope ID, USA) fitted with a 6.6 cm diameter polycarbonate core tube. Vesalea and Nopovois were cored in 2017 with a percussion corer (UWITEC, Mondsee, Austria) equipped with a 6.3 cm diameter polycarbonate tube. Unconsolidated upper sediment from these cores was subsampled at 1 cm intervals in the field and stored frozen in Whirl-Pak plastic bags (Nasco, Fort Atkinson, WI, USA). Analyses of lake surface sediment were restricted to the uppermost 1 or 2 cm of material. A hand trowel was used to collect the upper 1 cm of mangrove sediments in 2012. Samples were stored frozen in Whirl-Pak bags.

Water was collected from the surface of each lake and stored in screw-cap glass vials. Additional water samples were collected from adjacent streams and long-term precipitation integrators such as wells and rain cisterns when available. Samples were stored at 4 °C prior to analysis.

## 2.2 Leaf wax extraction and purification

Maloney et al. (2019) described lipid extraction, saponification, and column chromatography for all lake surface sediments except Dranoniveilomo, Vesalea, and Nopovois. Samples from Dranoniveilomo were processed following the protocol of Maloney et al. (2019). For all these lake sediments, the acid-containing fraction was eluted with 6 ml 4% acetic acid in diethyl ether from an aminopropyl gel column and the alkane-containing fraction was eluted with 6 ml hexane from a silica gel column. Lipid extraction, saponification, and column chromatography from Vesalea was described by Krentscher et al. (2019), and was identical for

the sample from Nopovois. Lipids from mangrove surface sediments were extracted and divided into compound classes using Si gel column chromatography as in Ladd and Sachs (2017).

For mangrove surface sediments, *n*-alkanes were purified from a Si gel hexane fraction by eluting 8 mL of 100% hexane over 0.5 g of $AgNO_3$-impregnated Si gel (10% by weight). For lake samples, the alkane fraction was urea adducted to isolate unbranched compounds. Fatty acids from lake sediments were methylated with 5% HCl in methanol for 12 hours at 70 °C, and saturated fatty acid methyl esters (FAMEs) were isolated by elution in 8 mL of 4:1 Hex/DCM over 0.5 g of $AgNO_3$-impregnated Si gel (10% by weight). Acid fractions were not analyzed from mangrove surface sediments. Purity and concentrations of *n*-alkanes from mangrove samples were assessed by gas chromatography – flame ionization detection (GC-FID) using the GC program and instrumentation described in Ladd and Sachs (2017). For lake samples, *n*-alkane and *n*-acid homologues were quantified using the same GC program and instrumentation described in Ladd et al. (2018).

### 2.3 $\delta^2H_{Wax}$ measurements

Samples were dissolved in hexane at a concentration suitable for hydrogen isotope analyses of *n*-$C_{29}$-alkane or *n*-$C_{28}$-acid when those compounds were sufficiently abundant for analysis by gas chromatography – isotope ratio mass spectrometry (GC-IRMS). $\delta^2H$ values of other baseline-resolved homologues with peak areas >15 Vs are also reported. For mangrove sediment samples, GC-IRMS analyses were conducted with the same GC program and isotopic referencing described in Ladd and Sachs (2017). Lake sediment samples were analyzed with the same GC program and isotopic referencing described in Ladd et al. (2018). Phthalic acid of known isotopic composition (Shimmelmann, Indiana University) was methylated to determine

185 $\delta^2H$ values of H added during methylation, which was corrected for using isotopic mass balance
186 (Lee et al., 2017).
187
188 2.4 Estimates of $\delta^2H_P$ values
189 Estimates of $\delta^2H_P$ values were extracted from different model products using latitude,
190 longitude, and elevation of each site. Model products included the Online Isotopes in
191 Precipitation Calculator (OIPC) version 3.2 (Bowen & Ravenaugh, 2003; IAEA/WMO, 2015;
192 Bowen, 2020), as well as isotope-enabled climate model contributions to the second Stable
193 Water Isotope Intercomparison Group (SWING2) from the CAM, ECHAM, GISS ModelE,
194 HadAM, isoGSM, LMDZ, and MIROC models (Sturm et al., 2010). OIPC estimated values were
195 obtained manually from the web interface ("OIPC mean annual $\delta^2H$"), and also by extraction
196 from the high-resolution spatial gridded data set using a bilinear smooth function to
197 accommodate the proximity of a given location to neighboring pixels and the $\delta^2H$ values from
198 those pixels ("OIPC extracted mean annual $\delta^2H$"). The multi-model mean annual precipitation
199 $\delta^2H$ value was calculated by averaging predicted values for all climate models that employed
200 spectral nudging (Yoshimura et al., 2008), which includes the ECHAM, GISS (nudged),
201 isoGSM, and LMDZ products.
202
203 2.5 Water $\delta^2H$ and $\delta^{18}O$ analyses
204 The isotopic composition of most lake and stream water samples were previously
205 analyzed and reported by Maloney et al. (2019). Water samples from the 2012 Micronesian field
206 campaign and from Lake Dranoniveilomo were analyzed by Cavity Ring Down Spectroscopy
207 (CRDS; Li-2130i, Picarro, Santa Clara, CA) using the same conditions and standards as in
208 Maloney et al. (2019). Additional water samples from the 2017 Vanuatu field campaign were

analyzed by Thermal Conversion/Elemental Analysis – Isotope Ratio Mass Spectrometry (TC/EA-IRMS; ThermoFisher Scientific, Bremen, Germany) using the same conditions and standards as in Newberry et al. (2017).

### 2.6 Pollen counts

Core samples for palynomorph analyses (including pollen and spores) were taken from within the upper portion of the sediment core to determine modern baseline vegetation differences among lakes. Each 1 $cm^3$ sample was processed using standard procedures (10% HCl, hot 10% KOH, and acetolysis) (Moore et al. 1991). Samples were spiked with exotic *Lycopodium clavatum* L. tablets to allow the palynomorph and charcoal concentrations to be calculated. Counts continued until reaching at least 100 terrestrial palynomorphs. Reference palynomorphs held in the Australasian Pollen and Spore Atlas (apsa.anu.edu.au/) assisted with identification. The vegetation types (primary, secondary, dryland herbs, wetland herbs, etc.) were determined from a regional synthesis of Pacific Island plant ecology (Mueller-Dombois & Fosberg 1998).

## 3 Results

### 3.1 $\delta^2H_{Wax}$ values in the tropical Pacific

$\delta^2H_{Wax}$ values from surface sediments in the tropical Pacific were not correlated with mean annual $\delta^2H_P$ values as calculated by the OIPC, nor with mean annual precipitation amount as estimated by the Global Precipitation Climatology Project (GPCP) (Adler et al., 2003) (Figure 2). The only lipids with significant correlations with $\delta^2H_P$ values were dinosterol (data from Maloney et al., 2019), *n*-$C_{16}$-acid, and *n*-$C_{18}$-acid, and the only significant correlations with the amount of mean annual precipitation were dinosterol, *n*-$C_{18}$-acid, *n*-$C_{17}$-alkane, and *n*-$C_{33}$-alkane.

In almost all cases, correlation coefficients were negative for the relationship between $\delta^2H_{Wax}$ and $\delta^2H_P$ values, and positive for the relationship between $\delta^2H_{Wax}$ values and mean annual precipitation. An exception was *n*-$C_{17}$-alkane, which, similarly to dinosterol, had $\delta^2H$ values that are negatively correlated with mean annual precipitation ($R = -0.95$; $p = 0.049$) and positively correlated with $\delta^2H_P$ values ($R = 0.95$; $p = 0.051$) (Figure 2). However, *n*-$C_{17}$-alkane was only abundant enough to measure its $\delta^2H$ values in four samples, making any assessment of these correlations tentative.

### 3.2 Tropical Pacific $\delta^2H$ values in the global context

Tropical Pacific $\delta^2H$ values of *n*-$C_{29}$-alkanes and *n*-$C_{28}$-acids (the most commonly measured leaf waxes in the literature) were in the range expected based on the global relationship between $\delta^2H_{Wax}$ and $\delta^2H_P$ values (Figure 3). Tropical Pacific *n*-$C_{29}$-alkane $\delta^2H$ values ranged from −177 to −139‰, while those of *n*-$C_{28}$-acid ranged from −175 to −119‰ (Table 1; Figure 3). Adding these new measurements to an updated global compilation of $\delta^2H_{Wax}$ values from all available surface sediment and soil data sets in non-marine settings (compilations from Liu & An, 2019 and McFarlin et al., 2019, as well as data sets from Nelson, 2013; Bakkelund et al., 2018; Feng et al., 2019; Goldsmith et al., 2019; Li et al., 2019; Wu et al., 2019; Lu et al., 2020; Struck et al., 2020; van der Veen et al., 2020) has minimal impact on the slope, y-intercept, or correlation coefficients for the global linear regression (Figure 3).

To compare new measurements from the tropical Pacific to the relationship defined by previously published values, we calculated their residual values from the global linear regression between $\delta^2H_{Wax}$ and $\delta^2H_P$ (excluding new tropical Pacific data). At most tropical Pacific locations, residuals from the global linear regression line were within ± 20‰, but were greater than this at 5 sites for *n*-$C_{29}$-alkane and 6 sites for *n*-$C_{28}$-acid (Table 1). Only two sites (Lake

Tagamaucia in Fiji and White Lake in Vanuatu) had residuals greater than 20‰ for both compounds.

We also contextualized variability in the tropical Pacific data relative to the global data set by randomly subsampling 17 values from the compiled data 4,000 times and comparing the correlation coefficient between $\delta^2H_{Wax}$ and $\delta^2H_P$ to the range in $\delta^2H_P$ values (Figure 4). None of these subsampled data sets had ranges in $\delta^2H_P$ values that were as small as the range in the tropical Pacific (smallest range for *n*-$C_{29}$-alkane = 59‰, for *n*-$C_{28}$-acid = 118‰), so we subsampled the compiled data again while restricting the maximum range to 100‰ (1,000 iterations each for the highest, lowest, and middle $\delta^2H_P$ values), 50‰ (200 iterations for each possible 50‰ range with maximum $\delta^2H_P$ values shifted by 10‰), and 35‰ (100 iterations for each possible 35‰ range with maximum $\delta^2H_P$ values shifted by 5‰). Correlation coefficients were typically high (>0.5) when the range of $\delta^2H_P$ values was greater than 100‰, and became increasingly scattered below this threshold (Figure 4). The relationship between the correlation coefficient and the range of $\delta^2H_P$ values in the tropical Pacific plotted within the range generated by random subsets. However, tropical Pacific correlation coefficients for both compounds were more than one standard deviation below the mean value of random sample sets with a $\delta^2H_P$ range between 30 and 35‰ (0.43 ± 0.28 for *n*-$C_{29}$-alkane; 0.22 ± 0.41 for *n*-$C_{28}$-acid) (Figure 4).

In addition to the OIPC, several water-isotope-enabled GCMs also provide estimates of mean annual $\delta^2H_P$ values. We extracted $\delta^2H_P$ values for all sites with surface sediment or soil $\delta^2H_{Wax}$ values from each climate model included in the Stable Water Isotope Intercomparison Group, Phase 2 (SWING 2) model comparison. For all models, global *n*-$C_{29}$-alkane and *n*-$C_{28}$-acid $\delta^2H$ values were positively correlated with $\delta^2H_P$ estimates (Figure 5). For *n*-$C_{29}$-alkane, $\delta^2H_{Wax}$ values were most highly correlated with $\delta^2H_P$ values obtained manually from the OIPC (R = 0.86). The lowest correlation was with $\delta^2H_P$ values from HadAM (R = 0.57) (Figure 5). For

280 *n*-$C_{28}$-acid, global $\delta^2H_{Wax}$ values were most highly correlated with $\delta^2H_P$ values extracted from the
281 CAM model (R = 0.91). The lowest correlation was with $\delta^2H_P$ values extracted from the high-
282 resolution spatial gridded OIPC data (R = 0.82) (Figure 5). The correlation coefficient obtained
283 manually from the OIPC (R = 0.86) was intermediate among the different models (Figure 5).
284
285 3.3 Pollen and spore spectra
286 Palynomorphs from most sites were indicative of human disturbance to the catchment
287 vegetation, as the dominant pollen types are from secondary forest taxa (Figure 6; Table 2).
288 When secondary forest vegetation was not most abundant, fern spores contributed more to the
289 palynomorph sum than any other plant group, except at Lake Hut, where primary forest taxa
290 were most abundant (Figure 6; Table 2). Although wetland plants covered more than 50% of the
291 surface water at three lakes (Onetahi Pond, Lake Tagamucia, and Veselea Pond), wetland herbs
292 and aquatic plants never contributed more than 23% of the observed pollen.
293 Pollen data are only available for three of the five sites where *n*-$C_{29}$-alkane residuals from
294 the global $\delta^2H_{Wax}$ vs. $\delta^2H_P$ relationship were less than −20‰ (Figure 6). In two of these
295 (Tagamaucia and White Lake), fern spores were abundant (59% and 39%, respectively) (Figure
296 6; Table 2). However, at the third site with an *n*-$C_{29}$-alkane residual less than −20‰ (Lake Hut),
297 fern spore concentrations were low and primary forest taxa palynomorphs were most abundant
298 (Figure 6; Table 2). Three sites had *n*-$C_{28}$-acid residuals from the global $\delta^2H_{Wax}$ vs. $\delta^2H_P$
299 relationship less than −20‰, of which two have pollen data (Tagamaucia and Dranoniveilomo).
300 Each of these had a high abundance of ferns and wetland plants (80% and 37%, respectively)
301 (Figure 6, Table 2). Three sites had *n*-$C_{28}$-acid residuals from the global $\delta^2H_{Wax}$ vs. $\delta^2H_P$ relations
302 that were greater than 20‰ (Figure 6). One of these, White Lake, had relatively high
303 contributions from ferns. The second, Harai Lake #1, does not have recent pollen data (the most

recent pollen sample is from 11 – 12 cm), but historically had high contributions from ferns (Table 2). The third, Nopovois, is dominated by secondary forest vegetation (54%) and does not have palynological features that clearly distinguish it from sites where *n*-$C_{28}$-acid $\delta^2H$ values adhere more closely to the global relationship (Figure 6; Table 2). Additionally, some sites with high contributions from ferns and wetland plants – Harai Lake #3, Lanoto'o, and Lake Otas – have $\delta^2H_{Wax}$ values close to the global relationship (Figure 6).

## 4 Discussion

Although the relationship between $\delta^2H_{Wax}$ and $\delta^2H_P$ values lacks any correlation for the tropical Pacific sites in isolation, the values fall within the global scatter around the linear regression of compiled literature values from surface sediments and soils (Figure 3; Table 1). In addition to adding recently published data, our global data set differs from two recent compilations by excluding marine sediments (in contrast to Liu and An, 2019), and including both soils and surface sediments (in contrast to McFarlin et al., 2019). Although leaf waxes in soils and sediments might have different sources and represent different timescales and catchment areas, there is no significant difference in the relationship between $\delta^2H_{Wax}$ and $\delta^2H_P$ for either compound (Figure 3c and 3d). The similarity between the soil and sediment compilations suggests that the transit history of leaf waxes from plant to deposition and subsequent preservation varies as much within archive type as it does between them.

The positive linear relationship between $\delta^2H_{Wax}$ and $\delta^2H_P$ values in the global compilation remains robust, with $R^2$ values of 0.74 for both *n*-$C_{29}$-alkane (n = 665) and *n*-$C_{28}$-acid (n = 242) (Figure 3). However, considerable scatter around the regression line exists globally and within the tropical Pacific. Large residuals are due to both uncertainty in the y-axis (variable $^2H/^1H$ fractionation between leaf waxes and water among plant types and environments, discussed in

section 4.1) and in the x-axis (mean annual $\delta^2H_P$ values and the water source used by plants, discussed in section 4.2).

### 4.1 Variable hydrogen isotope fractionation during leaf wax synthesis

Although global $\delta^2H_{Wax}$ values are well correlated with $\delta^2H_P$ values of mean annual precipitation (Figures 3, 5), several well-established factors contribute to variability in the net $^2H/^1H$ fractionation between plant waxes and precipitation ($\alpha_{Wax\text{-}P}$) (Sachse et al., 2012). Variations in $\alpha_{Wax\text{-}P}$ occur among plant functional types (Liu et al., 2006), between leaves and other plant organs (Gamarra & Kahmen, 2015), and with relative humidity (Tipple et al., 2015). Additionally, biosynthetic fractionation between leaf water and waxes can vary seasonally (Newberry et al., 2015), with environmental stresses (Ladd & Sachs, 2015), and with changes in plant metabolism (Cormier et al., 2018). Large differences in $\alpha_{Wax\text{-}P}$ can also exist among plant species growing at the same site (Feakins & Sessions, 2010; Sachse et al., 2012; Eley et al., 2014; He et al., 2020). With the current tropical Pacific data set we can only examine factors that might relate to differences among different types of plants, and not factors that can occur within a single plant, such as metabolic state. We examine three plant groups – mangroves, aquatic plants, and ferns –whose contributions may impact community $\delta^2H_{Wax}$ values. By comparing pollen distributions and information about surrounding vegetation at each site with the residuals between $\delta^2H_{Wax}$ values and the global calibration line (Figure 6), we demonstrate that changes in vegetation inferred from pollen cannot consistently explain anomalous $\delta^2H_{Wax}$ values in tropical Pacific surface sediments.

#### 4.1.1 Mangroves

Mangroves are woody plants that grow in brackish to hypersaline water. They contribute large amounts of organic matter to coastal sediments in the tropics and subtropics (Alongi, 2014). Because mangroves discriminate more against $^{2}H$ as salinity increases (Ladd & Sachs, 2012; He et al., 2017; Ladd & Sachs, 2017), they should have lower $\delta^{2}H_{Wax}$ values than nearby freshwater plants. This relationship was recently observed in the Florida Everglades, where mangroves have $\delta^{2}H_{Wax}$ values ~50‰ lighter than those from nearby freshwater trees, despite equivalent $\delta^{2}H_{P}$ values (He et al., 2020). Significant contributions of mangrove leaf waxes in coastal areas in the tropical Pacific could result in sedimentary $\delta^{2}H_{Wax}$ values that fall below the global calibration line.

Several of the lakes in our calibration set were located in coastal areas, but only one, Dranoniveilomo, had brackish water and mangroves growing directly in its periphery. In this lake *n*-$C_{28}$-acid is significantly depleted relative to the global calibration, but *n*-$C_{29}$-alkane is not (Table 1). Despite the abundant mangroves around Dranoniveilomo, barely any mangrove pollen was found in the sediment, which may reflect different transport mechanisms and catchment areas for leaf waxes and pollen (Table 2). Two coastal lakes in Vanuatu (Otas and Waérowa East) have the highest amounts of mangrove pollen observed in all examined surface sediments (~15%; Figure 6; Table 2). In Lake Otas, $\delta^{2}H_{Wax}$ values are close to the values predicted by the global relationship (Table 1). In Lake Waérowa East, they are slightly higher than expected (Table 1), opposite to the expected impact of significant mangrove leaf wax contributions. These data suggest that mangrove leaf waxes are not an important influence on $\delta^{2}H_{Wax}$ values in tropical Pacific lake sediments included in this study.

Likewise, Micronesian mangrove swamp surface sediments had $\delta^{2}H_{Wax}$ values that were consistent with the global linear regression (Table 1; Figure 3). Additionally, there was little spatial variability in $\delta^{2}H_{Wax}$ values throughout each individual mangrove swamp, with 5‰

standard deviations among samples within a single swamp (Table 1). This homogeneity occurred even though samples were collected from sites with surface water salinity ranging from 0-31 at the time of collection. Surface water salinity was dynamic throughout these mangrove swamp surveys, varying temporally and spatially with tides and rain events. Individual mangrove trees with large root networks therefore had access to water with a wide range of salinities and may have opportunistically taken up relatively fresh water that was ultimately used in leaf wax synthesis. Preferential uptake of fresher water by mangroves has been observed previously (Santini et al., 2015; Reef et al., 2015), and could result in all mangroves throughout a swamp using water with similar salinity and isotopic composition, consistent with the surface sediment $\delta^2H_{Wax}$ values observed in transects from Micronesian mangrove swamps.

#### 4.1.2 Aquatic plants

Some of the lakes included in the tropical Pacific survey were partially or completely covered by floating aquatic vegetation (Table 1). Since aquatic plants at diverse sites tend to have lower alkane $\delta^2H_{Wax}$ values than nearby terrestrial plants (Chikaraishi & Naraoka, 2003; Gao et al., 2011; Dion-Kirschner et al., 2020; He et al., 2020), differing relative contributions of leaf waxes from aquatic plants could also reduce sedimentary $\delta^2H_{Wax}$ values. There are a few reasons why aquatic plants may have relatively low $\delta^2H_{Wax}$ values. First, when a lake is mostly covered by water lilies or similar aquatic vegetation, there is a physical barrier to evaporation of lake water, and it may therefore maintain a $\delta^2H$ signal similar to that of precipitation, rather than becoming enriched in $^2H$ due to transpiration, as is the case for leaves exposed to air (Kahmen et al., 2013; Cernusak et al., 2016). Second, it is possible that aquatic plants may exhibit greater biosynthetic fractionation between leaf water and leaf lipid. However, existing investigations of

397 $\delta^2H_{Wax}$ values in submerged aquatic plants suggest this is only likely at high salinity, while plants
398 grown in freshwater display similar $\alpha_{Wax\text{-}P}$ values to other plants (Aichner et al, 2017).

399 High contributions from aquatic plants could explain why $\delta^2H_{Wax}$ values at Tagamaucia in
400 Fiji, which is covered in floating sedge islands (Southern et al., 1986), were very $^2$H-depleted
401 relative to the global calibration line (Table 1). However, this relationship was not consistent in
402 all lakes covered by aquatic plants. For example, Lake Veselea in Vanuatu is completely covered
403 by mats of aquatic plants (primarily *Persicaria* cf. *attenuata*, *Salvinia molesta*, and *Calystegia*
404 *soldanella*), yet $\delta^2H_{Wax}$ values from its sediment fell close to the global calibration line (Table 1).
405 Additionally, pollen from wetland herbs and aquatic plants is not consistently associated with
406 large or small residuals from the global calibration line (Figure 6). Aquatic plants may have
407 minimal influence on sedimentary $\delta^2H_{Wax}$ values because submerged plants are not at risk of
408 desiccation and therefore have little need for the moisture barrier provided by long-chain leaf
409 waxes. They therefore tend to have low concentrations of these compounds (Ficken et al., 2000;
410 Dion-Kirschner et al., 2020; He et al., 2020). Overall, our results suggest that increased presence
411 of aquatic plants does not unequivocally result in decreased $\delta^2H_{Wax}$ values in tropical Pacific lake
412 sediments.

413

414 4.1.3 Ferns

415 Assessments of $\delta^2H_{Wax}$ values from ferns are limited, but previous studies show that ferns
416 have similar $\alpha_{Wax\text{-}P}$ values to many other plant taxa, including lycopods, gymnosperms, eudicots,
417 and magnoliids (Gao et al., 2014). We therefore had no expectation that sites with large
418 sedimentary contributions of leaf waxes from ferns would diverge from the global $\delta^2H_{Wax}$-$\delta^2H_P$
419 linear regression. However, some of the sites with the largest residuals relative to the global
420 regression line had palynomorph spectra characterized by large contributions of fern spores. This

421 was particularly true at Lake Tagamaucia in Fiji and White Lake in Vanuatu, and to a lesser
422 extent in Fiji's Lake Dranoniveilomo (Table 1; Figure 6). However, high accumulation of fern
423 spores did not universally correspond to low $\delta^2H_{Wax}$ values, for example at Lake Lanoto'o in
424 Samoa and Harai Lakes #1 and #3 in the Solomon Islands (Tables 1 and 3; Figure 6). Of these,
425 *n*-$C_{28}$-acid $\delta^2H$ values from the Harai Lakes were much higher than the predicted values from the
426 global regression fit, in direct contrast to the Fijian lakes and White Lake (Table 1; Figure 6).
427 Additionally, Lake Hut in New Caledonia had the largest *n*-$C_{29}$-alkane residual for any site with
428 pollen data, but did not have much fern pollen (Figure 6). Overall, this suggests that relative
429 contributions of leaf waxes from ferns do not have predictable effects on sedimentary $\delta^2H_{Wax}$
430 values. Nevertheless, a shift in $\delta^2H_{Wax}$ values that coincides with a change in the relative
431 abundance of fern spores in a down-core record may indicate a change in organic matter sources
432 rather than a change in $\delta^2H_P$ values.
433
434 4.2 Uncertainty in $\delta^2H_P$ values
435 Variability in $\alpha_{Wax\text{-}P}$ contributes to uncertainty in the y-axis in the relationship between
436 $\delta^2H_{Wax}$ and $\delta^2H_P$ (Figure 3). However, unlike most proxy systems, the x-axis calibration target is
437 poorly constrained and likely accounts for a large portion of the linear regression residuals
438 between $\delta^2H_{Wax}$ and $\delta^2H_P$ values in the tropical Pacific. $\delta^2H_P$ values are not constant throughout
439 the year, and water from different seasons has different residence times in soil, meaning that the
440 $\delta^2H$ values of water used by plants is typically not equal to mean annual $\delta^2H_P$ values (Brinkmann
441 et al., 2018). Additionally, $\delta^2H_P$ values from the OIPC represent climatological means, but $\delta^2H_P$
442 values vary interannually and seasonally. The time period captured by a surface sediment sample
443 (typically a few years to two decades; see Maloney et al., 2019 for sediment accumulation rates
444 at most sites) may differ considerably from the long-term mean. Finally, the robustness of mean

445 annual estimates provided by the OIPC varies spatially among geographic settings due to the
446 uneven density of $\delta^2H_P$ observations (IAEA/WMO, 2015).

447 Limited $\delta^2H_P$ data from some sites in the tropical Pacific mean that $\delta^2H_P$ values calculated
448 using OIPC have large uncertainties (Table 1). This is especially problematic for sites in the
449 southeastern portion of the region, since there are no observations of $\delta^2H_P$ values from the
450 Solomon Islands, Vanuatu, or New Caledonia in the GNIP database. 95% confidence intervals
451 for $\delta^2H_P$ values from sites in Vanuatu are as large as 76‰, considerably larger than the overall
452 range in $\delta^2H_P$ values (~30‰) and the range in measured $\delta^2H_{Wax}$ values (~40‰ for *n*-$C_{29}$-alkane
453 and ~55‰ for *n*-$C_{28}$-acid) in the Pacific (Table 1; Figure 3). For other sites, such as those in
454 Micronesia, OIPC uncertainties may add false confidence to predicted values, as these can be
455 based on a limited number of GNIP observations from several decades ago. For example, the
456 Yap GNIP station has 65 observations collected from 1968 to 1976, and the station on Chuuk
457 (Truk) has 72 observations collected between 1968 and 1977 (IAEA/WMO, 2015).
458 Climatological means calculated from these data may not be representative of conditions when
459 surface sediment leaf waxes in this study formed. This uncertainty in the independent variable
460 likely contributes to the lack of a regional correlation between $\delta^2H_{Wax}$ and $\delta^2H_P$ values (Figure 3).

461 An alternative approach for estimating mean annual $\delta^2H_P$ values is to use water-isotope-
462 enabled GCMs (Sturm et al., 2010; Conroy et al., 2013; Steen-Larsen et al., 2017). These
463 estimates of $\delta^2H_P$ values have not typically been used in $\delta^2H_{Wax}$ calibration studies. Because
464 some of the western Pacific $\delta^2H_P$ values derived from OIPC had such large uncertainties, we
465 assessed whether scatter in the global relationship between $\delta^2H_{Wax}$ and $\delta^2H_P$ could be reduced by
466 using isotope-enabled GCMs to estimate $\delta^2H_P$ values (Figure 5).

467 In general, $\delta^2H_{Wax}$ values from *n*-$C_{28}$-acid are better correlated with $\delta^2H_P$ values generated
468 by isotope-enabled GCMs than $\delta^2H_{Wax}$ values from *n*-$C_{29}$-alkane. This difference may be due to
469 the distinct spatial distributions of the two calibration data sets, with fatty acid $\delta^2H$ values almost
470 exclusively limited to North America (Figure 1). Sites from which *n*-alkane $\delta^2H$ values are
471 available are more numerous, more globally distributed, and include many measurements from
472 the Himalayas and Tibetan Plateau (Figure 1). Here, steep elevation gradients may make $\delta^2H_P$
473 vary on spatial scales that are smaller than the resolution of most models, and fluvial and aeolian
474 processes may transport waxes between regions with distinct $\delta^2H_P$ values. Overall, our analysis
475 does not suggest any structural limitations to using the OIPC to estimate $\delta^2H_P$ values for proxy
476 calibration. However, the limited $\delta^2H_P$ measurements from the tropical Pacific and resulting large
477 uncertainties in modern estimates from the OIPC or isotope-enabled GCMs remains a
478 considerable challenge for assessing the fidelity of $\delta^2H_{Wax}$ values in this region.

479 In particular, the orographic effects of mountainous islands may not be adequately captured
480 by either the OIPC or isotope-enabled GCMs, causing particular challenges determining the
481 appropriate calibration target for water isotope proxies. For example, the highest peaks on the
482 island of Espiritu Santo in Vanuatu are nearly 2000 m above sea level. With prevailing winds
483 from the east, the west coast sits in the rain shadow of the mountains and is significantly drier
484 than the eastern part of the island (Terry, 2011). However, the only long-term weather station for
485 the island is located at Pekoa airport in the southeast corner of the island, and there are no local
486 GNIP stations. Therefore, minimal local data is available to inform precipitation isotope models.
487 The OIPC predicts equivalent $\delta^2H_P$ values for sites on opposite coasts of Espiritu Santo, and
488 predicted $\delta^2H_P$ values from water-isotope-enabled GCMs on each coast are within a few ‰ of
489 each other. However, the leeward western sites should have lighter $\delta^2H_P$ values than the eastern
490 sites that receive rain from more marine air masses (Scholl et al., 1996, 2007). This expectation

491 is supported by the $\delta^2H$ values of lake and stream waters collected during our field campaigns,
492 which are depleted by 20 – 40 ‰ on the leeward western side of the island compared to the
493 windward east coast (Data Set S2).
494
495 4.3 Contrasts with $\delta^2H$ values of non-leaf wax lipids
496 In addition to the longer chain *n*-alkane and *n*-alkanoic acids that are primarily derived
497 from higher plant waxes, we also measured $\delta^2H$ values from several compounds of mixed or
498 primarily algal sources. These compounds are typically found in sedimentary records along with
499 leaf waxes, and the different controls on their $\delta^2H$ values offer the opportunity to more
500 completely resolve sources of down-core variability in $\delta^2H_{Wax}$ values. Here we discuss lipids
501 from algal sources, and ubiquitous compounds produced by most organisms.
502
503 4.3.1 Algal lipids
504 Unlike $\delta^2H_{Wax}$ values, $\delta^2H$ values of algal biomarkers are well correlated with tropical
505 Pacific $\delta^2H_P$ values and mean annual precipitation (Figure 2). This is particularly the case for
506 dinosterol (Maloney et al., 2019), which is primarily produced by dinoflagellates (Volkman,
507 2003). The $\delta^2H$ values of *n*-$C_{17}$-alkane, which is primarily derived from algae (Cranwell et al.,
508 1987; Meyers, 2003), were also highly correlated with $\delta^2H_P$ values (consistent with Sachse et al.,
509 2004) and inversely correlated with mean annual precipitation (Figure 2). An inverse correlation
510 between the amount of mean annual precipitation and $\delta^2H_P$ values (and therefore $\delta^2H$ values of
511 lipids that track $\delta^2H_P$) is expected in a low-latitude maritime regions where the amount effect
512 plays a strong role in determining the isotopic composition of rain (Dansgaard, 1964; Rozanski
513 et al., 1993; Kurita et al., 2009).

One reason why $\delta^2H$ values from the algal biomarkers are better correlated with $\delta^2H_P$ values than $\delta^2H_{Wax}$ values might relate to the source water used by each type of organism. Leaf waxes from higher plants growing on land may reflect a temporal bias, as monthly OIPC $\delta^2H_P$ values can differ by up to 40‰ at the tropical Pacific sites. Higher plants primarily produce leaf waxes soon after setting new leaves, meaning that there may be a seasonal bias in the $\delta^2H_P$ signal that is transferred to their waxes (Tipple et al., 2013; Freimuth et al., 2017). If algae are productive throughout the year, they may better integrate annual precipitation, therefore resulting in algal lipids that more closely track mean annual $\delta^2H_P$ values.

Another reason why algal biomarkers may track $\delta^2H_P$ better than leaf waxes is that they come from a more limited range of potential sources. In addition to the range of plant sources for leaf waxes discussed in section 4.1, many of the mid-chain and relatively long-chained acetogenic compounds, including *n*-$C_{29}$-alkane and *n*-$C_{28}$-acid, can be derived from a mix of terrestrial and aquatic plants (Bush & McInerney, 2013; Andrae et al., 2020; Dion-Kirschner et al., 2020). *n*-$C_{28}$-acid can also be partially derived from microalgal sources (Volkman, 1980; van Bree et al., 2018). Therefore the leaf waxes may represent variable aquatic and terrestrial contributions, while the algal compounds are always aquatically sourced.

Finally, the spatial variability integrated by each type of compound could explain the different trends in their $\delta^2H_{Wax}$ values. Algal lipids are produced within the relatively confined space of the lake or pond overlaying the sediments in which they accumulate. Leaf waxes can be derived from plants growing adjacent to their depocenter, but also from further afield in the catchment, and the relative size of the catchment area can differ among water bodies. Additionally, > 20% of leaf waxes accumulating in sediment can come from aerosols, which can be transported long distances and have $\delta^2H$ values distinct from local vegetation (Conte et al., 2003; Gao et al., 2014; Nelson et al., 2017; Nelson et al., 2018). Leaf wax aerosols from very

distant sites may have more impact on lake sediments on islands than on continents, since there is a relatively smaller contiguous land area to contribute regional and local waxes. On the other hand, the overall contribution of local leaf waxes may be significantly higher on small islands where all non-local leaf waxes must be carried great distances.

4.3.2 Generic fatty acids

In contrast to the algal specific biomarkers dinosterol and *n*-$C_{17}$-alkane, $\delta^2H$ values of *n*-$C_{16}$ and *n*-$C_{18}$ fatty acids were positively correlated with mean annual precipitation and negatively correlated with $\delta^2H_P$ (Figure 2). These shorter chain fatty acids are synthesized by most organisms, but are frequently attributed to algal sources in aquatic sediments (Huang et al., 2004; Li et al. 2009). Heterotrophic and chemoautotrophic microbes produce short-chain fatty acids that can have $\delta^2H$ values that differ by several hundred ‰ from those of photoautotrophs grown in similar water (Zhang et al., 2009; Heinzelmann et al., 2015). However, other than in microbial mats (Osburn et al., 2011), sedimentary *n*-$C_{16}$ and *n*-$C_{18}$ fatty acids typically have fractionation factors consistent with values from photoautotrophs in culture (Li et al, 2009; Zhang et al., 2009; Heinzelmann et al., 2018). In our tropical Pacific data set, fractionation factors between lake water and *n*-$C_{16}$ and *n*-$C_{18}$-acids ($\alpha_{Lipid\text{-}Water} = (^2H/^1H)_{Lipid}/ (^2H/^1H)_{Water}$) ranged from 0.773 to 0.920. This large range in $\alpha_{Lipid\text{-}Water}$ values is consistent with observations of cultures of different types of algae (Zhang and Sachs, 2007; Zhang et al., 2009; Heinzelmann et al., 2015). The $\delta^2H$ values of the *n*-$C_{16}$ and *n*-$C_{18}$-acids in our data set could be influenced by variable contributions from non-photoautotrophs, but could also vary due to differing contributions from different types of algae. In either case, it seems likely that $\delta^2H$ values of these compounds reflect ecology more than hydroclimate, and their negative correlations with $\delta^2H_P$ values in our sample set may be a coincidence. Dinosterol and *n*-$C_{17}$-alkane are sourced from a

smaller range of organisms than the near ubiquitous *n*-$C_{16}$ and *n*-$C_{18}$-acids (Cranwell et al., 1987; Meyers, 2003; Volkman, 2003), which could make their $\delta^2H$ values more directly related to those of lake water.

### 4.4 Implications for paleoclimate reconstructions in the tropical Pacific

Although $\delta^2H_{Wax}$ values are strongly linearly correlated with $\delta^2H_P$ values on a global scale (Figure 3), the large residuals in this relationship indicate that caution should be applied before interpreting relatively small down-core changes in $\delta^2H_{Wax}$ values as hydroclimate changes. However, our data do not suggest that there are clear links between vegetation source (as indicated by palynological analyses) and residuals from the global $\delta^2H_{Wax}$-$\delta^2H_P$ relationship (Figure 6). Rather, one of the largest challenges for interpreting sedimentary $\delta^2H_{Wax}$ values in the tropical Pacific are uncertainties associated with modern estimates of $\delta^2H_P$ values, given the limited spatial and temporal available of modern observations. Recent isotope modeling work has helped constrain the processes that control $\delta^2H_P$ values in this dynamically important region (Conroy et al., 2016; Konecky et al., 2019). Continued effort in this regard is necessary to robustly interpret proxies $\delta^2H_P$ values, whether they are derived from $\delta^2H_{Wax}$ values or from other archives such as speleothems.

The expected inverse correlation between precipitation amount and OIPC-derived $\delta^2H_P$ values in the tropical Pacific, and the correlations between these variables and algal lipid $\delta^2H$ values (Maloney et al., 2019), suggest that the uncertainty in $\delta^2H_P$ values cannot be solely responsible for the poor correlations associated with $\delta^2H_{Wax}$ values (Figure 2). Rather, factors besides $\delta^2H_P$ values that influence $\delta^2H_{Wax}$ values (variations in seasonality, catchment scales, contributions from organs other than leaves and/or from aquatic sources, or changes in biosynthetic fractionation) result in residuals that are on the order of ±25‰ in the tropical Pacific

and elsewhere (Figure 3). Any calibration of $\delta^2H_{Wax}$ values spanning a relatively small range of $\delta^2H_P$ values (like the 32‰ range studied here) is likely to have a poor correlation between the two variables (Figure 4). Correlation coefficients for the tropical Pacific are within the distribution generated by randomly subsampling the global data set while limiting the range in $\delta^2H_P$ to 35‰, but fall towards the low end of this range, more than 1 standard deviation below the mean correlation coefficient (Figure 4).

Regional calibrations are expected to have stronger than average correlations by constraining some variables that contribute to scatter in the global relationship between $\delta^2H_P$ and $\delta^2H_{Wax}$ values. However, the new data from the tropical Pacific exceed a regional scale in many ways, spanning a distance of ~8500 km, larger than even continental-scale studies (e.g., Sachse et al., 2004). The islands included range from low-lying atolls to mountainous volcanoes. The sites differ in seasonality of precipitation, vulnerability to tropical storms, sensitivity to El Niño−Southern Oscillation events, and biodiversity, all of which may impact $\delta^2H_{Wax}$ values. The diversity of sites, uncertainty in local estimates of $\delta^2H_P$ values, and small $\delta^2H_P$ signal relative to the noise in the global calibration, make it unsurprising that $\delta^2H_{Wax}$ values are not correlated with $\delta^2H_P$ values within the tropical Pacific. However, it is encouraging that tropical Pacific $\delta^2H_{Wax}$ values fall within the expected range, and do not have abnormally large residuals from the global calibration line. Together, these results suggest that the processes determining $\delta^2H_{Wax}$ values in tropical Pacific lake and swamp sediments are not fundamentally different than elsewhere.

The scatter in the global relationship between $\delta^2H_P$ and $\delta^2H_{Wax}$ (Figure 3) suggests that down-core changes as large as ~50‰ at any location could be driven by factors other than $\delta^2H_P$ values. In practice, at a single site where many variables that contribute to scatter among sites are constant, the threshold for detecting changes in $\delta^2H_P$ values may be significantly smaller. Detailed processed-based studies at the catchment scale (Freimuth et al., 2019, 2020; Dion-

Kirschner et al., 2020) may be more useful for constraining sedimentary $\delta^2H_{Wax}$ than additional large-scale calibration efforts.

Hydroclimate-driven interpretations of changes in sedimentary $\delta^2H_{Wax}$ values will be most robust when supported by independent lines of proxy evidence, such as $\delta^2H$ values of more source specific biomarkers like dinosterol (Smittenberg et al., 2011; Nelson & Sachs, 2016; Richey & Sachs, 2016; Sachs et al., 2018), changes in grain size distributions (Conroy et al., 2008), or changes in the elemental composition of inorganic sediments (Sear et al 2020; Higley et al., 2018). Continued refinement of a multi-proxy toolbox that includes sedimentary $\delta^2H_{Wax}$ values offers the best path to confidently reconstructing past hydrologic change.

## 5 Conclusions

$\delta^2H_{Wax}$ values from surface sediments from 19 lakes and four swamps on 15 islands throughout the tropical Pacific fall within the overall range of values expected based on a global compilation surface sediment measurements ($R^2$ = 0.74 for both *n*-$C_{29}$-alkane (n = 665) and *n*-$C_{28}$-acid (n = 242)), and the residuals around the global linear regression between $\delta^2H_{Wax}$ and $\delta^2H_P$ are similar in the tropical Pacific and global data sets. Nevertheless, within the tropical Pacific there is no significant correlation between $\delta^2H_{Wax}$ and $\delta^2H_P$ values. The lack of correlation regionally is at least partly due to the large uncertainties in $\delta^2H_P$ values derived from reanalysis data and cannot be ascribed to different vegetation sources within and surrounding the lakes in this study, as deduced from pollen assemblages.

To a first order on a global scale, $\delta^2H_{Wax}$ values are clearly influenced by $\delta^2H_P$ values, but the $\delta^2H_P$ signal spanning the tropical Pacific remains small relative to the noise in the current global calibration. The global $\delta^2H_{Wax\text{-}P}$ calibration remains limited by uncertainties in both the x- and y-axes, and could be improved by better constraints on $\delta^2H_P$ values. As in other locations,

large changes in $\delta^2H_{Wax}$ in sediments from tropical Pacific islands may be caused by variables other than $\delta^2H_P$, and could be improved by more catchment-scale, processed-based studies. In particular, interpretations need to consider the possible effects of changing source, growth conditions, and delivery of leaf waxes to sediments. When possible, $\delta^2H_{Wax}$ values should be paired with $\delta^2H$ values of more source-specific compounds such as dinosterol, which can help distinguish changes in water isotopes from changes in other factors that affect $\alpha_{Wax\text{-}P}$ values. As is the case for all paleoclimate proxies, interpretations of $\delta^2H_{Wax}$ values are most robust in a multiproxy context.

## Acknowledgments, Samples, and Data

Funding was provided by a Swiss National Science Foundation grant to ND (Grant Nr. PP00P2_163782), a National Science Foundation grant to JPS (Grant No. 1502417), a NERC grant to DAS (NE/N00674/1), and an Australian Research Council grant to MP (DP0985593). Carsten Schubert hosted NL for laboratory work and provided necessary instrumentation. Nichola Strandberg provided pollen data from Lake Hut. Christiane Krentscher helped with sample processing in addition to those acknowledged by Maloney et al. (2019). Julie Richey and many others helped with sample collection, as acknowledged by Maloney et al. (2019) and Krentscher et al. (2019). All data associated with this manuscript is freely available in the ETH data repository (doi: 10.3929/ethz-b-000412154).

## Figure captions

**Figure 1** Global distribution of leaf wax samples from surface sediments and soils. The left panel shows the locations for *n*-$C_{29}$-alkane (665 sites); the right panel shows the locations for *n*-$C_{28}$-acid (242 sites). Background shading represents annual mean $\delta^2H_P$ values from the Online Isotopes in Precipitation Calculator (OIPC) (Bowen & Ravenaugh, 2003; IAEA/WMO, 2015; Bowen, 2020). OIPC does not produce spatial data sets over marine areas, therefore shading is limited to continents.

**Figure 2:** Correlation coefficients of linear regressions of $\delta^2H$ values of all analyzed compounds relative to $\delta^2H_P$ values (blue circles) and mean annual precipitation (pink diamonds) in the tropical Pacific. Filled symbols represent significant correlations at the 95% confidence level. Mean annual precipitation is from the Global Precipitation Climatology Project (GPCP) and $\delta^2H_P$ values are from the OIPC. Compounds are grouped by source (algal, general, or plant waxes, with increasingly likely terrestrial plant sources associated with longer chain lengths). Dinosterol $\delta^2H$ data is from Maloney et al. (2019), all other lipid $\delta^2H$ data from this study. Individual measurements are included in Data Set S1.

**Figure 3** $\delta^2H$ values of (a, c) *n*-$C_{29}$-alkane and (b, d) *n*-$C_{28}$-acid from surface sediments and soils plotted relative to OIPC-derived $\delta^2H_P$ values, color-coded by region (a, b), and sample type (c, d). In panels a and b, red diamonds are lakes from the SPCZ region and green squares are mangrove swamps in Micronesia (this study), both plotted with error bars. X-axis error bars represent 95% confidence intervals of OIPC values. Y-axis error bars represent 1 standard deviation of measurements from replicate samples from the same lake or swamp and are typically smaller than the marker size. Circles are global values compiled from the literature, color-coded by region. X-axis error bars are not shown for previously published data points, and average 5.2‰ for sites outside the tropical Pacific. Regression statistics in (a) and (b) are shown with and without new Pacific data. Globally compiled data (including tropical Pacific values) do not differ significantly between soils and lacustrine sediments for either (c) *n*-$C_{29}$-alkane or (d) *n*-$C_{28}$-acid. Shading around linear regressions represents 95% confidence intervals.

**Figure 4** Correlation coefficients of random subsamples of 17 values from the global compilation surface sediment and soil of (a) *n*-$C_{29}$-alkane and (b) *n*-$C_{28}$-acid $\delta^2H$ values plotted relative to range of $\delta^2H_P$ values. Subsampled data were taken from the full data set and from restricted $\delta^2H_P$ ranges as described in the text. Correlation coefficients for the global compilation and each continent are plotted for comparison.

**Figure 5** Correlation plots of $\delta^2H$ values from the global compilation of surface sediments and soils relative to the $\delta^2H_P$ values from various models (described in section 2.4). Numbers, colors, and the widths of the ellipses correspond to correlation coefficients (R values).

**Figure 6** Pollen distributions from surface or near surface sediments in tropical Pacific lake samples plotted relative to residuals from the global $\delta^2H_{Wax} - \delta^2H_P$ calibration line for (a) *n*-$C_{29}$-alkane and (b) *n*-$C_{28}$-acid. Square and triangle symbols are used to distinguish among multiple sites with the same residual values.

## References

Adler R. F., Huffman, G. J., Chang, A., Ferraro, R., Xie, P.-P., Janowiak, J., et al. (2003). the version-2 Global Precipitation in Climatology Project (GPCP) monthly precipitation analysis (1979 -- Present). Journal of Hydrometeorology, 4(6), 1147-1167.

Aichner, B., Herzschuh, U., Wilkes, H., Vieth, A., Böhner, & J. (2010). δD values of n-alkanes in Tibetan lake sediments and aquatic macrophytes–A surface sediment study and application to a 16 ka record from Lake Koucha. *Organic Geochemistry*, *41*(8), 779-790. https://doi.org/10.1016/j.orggeochem.2010.05.010

Aichner, B., Hilt, S., Périllon, C., Gillefalk, M., & Sachse, D. (2017). Biosynthetic hydrogen isotopic fractionation factors during lipid synthesis in submerged aquatic macrophytes: Effect of groundwater discharge and salinity. *Organic Geochemistry*, *113*, 10-16. https://doi.org/10.1016/j.orggeochem.2017.07.021

Alongi D. M. (2014). Carbon cycling and storage in mangrove forests. *Annual Review of Marine Science*, *6*, 195-219. https://doi.org/10.1146/annurev-marine-010213-135020

Andrae, J. W., McInerney, F. A., & Kale Sniderman, J. M. (2020). Carbon isotope systematics of leaf wax *n*-alkanes in a temperate lacustrine depositional environment. *Organic Geochemistry*, *150*, 104121. https://doi.org/10.1016/j.orggeochem.2020.104121

Bai, Y., Fang, X., Gleixner, G., & Mügler, I. (2011). Effect of precipitation regime on dD valuesügler, I., 2011. Effect of precipitation regime on δD values of soil n-alkanes from elevation gradients – implications fort he study of paleoelevation. *Organic Geochemistry*, *42*(7), 838-845. https://doi.org/10.1016/j.orggeochem.2011.03.019

Bakkelund, A., Porter, T. J., Froese, D. G., & Feakins, S. J. (2018). Net fractionation of hydrogen isotopes in *n*-alkanoic acids from soils in the northern boreal forest. *Organic Geochemistry*, *125*, 1-13. https://doi.org/10.1016/j.orggeochem.2018.08.005

Bowen, G. J. (2020). The Online Isotopes in Precipitation Calculator, version 3.1. http://www.waterisotopes.org.

Bowen, G. J., & Ravenaugh, J. (2003). Interpolating the isotopic composition of modern meteoric precipitation. *Water Resources Research*, *39*(10), 1-13. https://doi.org/10.1029/2003WR002086

Bowen, G. J., Cai, Z., Fiorella, R. P., & Putman, A. L. (2019). Isotopes in the water cycle: regional- to global-scale patterns and applications. *Annual Review of Earth and Planetary Sciences*, *47*, 453-479. https://doi.org/10.1146/annurev-erath-053018-060220

Brinkmann, N., Seeger, S., Weiler, M., Buchmann, N., Eugster, W., & Kahmen, A. (2018). Employing stable isotopes to determine the residence times of soil water and the temporal origin of water taken up by *Fagus sylvatica* and *Picea abies* in a temperate forest. *New Phytologist*, *219*(4), 1300-1313. https://doi.org/10.1111/nph.15255

Brown, J. R., Moise, A. F., & Delage, F. P. (2011). Changes in the South Pacific Convergence Zone in IPCC AR4 future climate projections. *Climate Dynamics*, *39*, 1-19. https://doi.org/10.1007/s00382-011-1192-0

Bush, R. T., & Mcinerney, F. A. (2013). Leaf wax n-alkane distributions in and across modern plants: implications for paleoecology and chemotaxonomy. *Geochimica et Cosmochimica Acta*, *117*, 161-179. https://doi.org/10.1016/j.gca.2013.04.016

Calvo, E., Marshall, J. F., Pelejero, C., McCulloch, M. T., Gagan, M. K., & Lough, J. M. (2007). Interdecadal climate variability in the Coral Sea since 1708 A.D. *Palaeogeography, Palaeoclimatology, Palaeoecology*, *248*(1-2), 190-201. https://doi.org/10.1016/j.palaeo.2006.12.003

Cernusak, L. A., Barbour, M. M., Arndt, S. K., Cheesman, A. W., English, N. B., Feild, T. S., et al. (2016). Stable isotopes in leaf water of terrestrial plants. *Plant, Cell and Environment*, *39*(5), 1087-1102. https://doi.org/10.1111/pce.12703

Chikaraishi Y., & Naraoka H. (2003). Compound-specific δD-$\delta^{13}$C analyses of n-alkanes extracted from terrestrial and aquatic plants. *Phytochemistry*, *63*(3), 361–371. https://doi.org/10.1016/S0031-9422(02)00749-5

Conroy, J. L., Cobb, K. M., & Noone, D. (2013). Comparison of precipitation isotope variability across the tropical Pacific in observations and SWING2 model simulations. *JGR Atmospheres*, *118*(11), 5867-5829. https://doi.org/10.1002/jgrd.50412

Conroy, J. L., Noone, D., Cobb, K. M., Moerman, J. W., & Konecky, B. L. (2016). Paired stable isotopologues in precipitation and vapor: A case study of the amount effect within western tropical Pacific storms. *JGR Atmospheres*, *121*(7), 3290-3303. https://doi.org/10.1002/2015JD023844

Conte, M. H., Weber, J. C., Carlson, P. J., & Flanagan, L. B. (2003). Molecular and carbon isotopic composition of leaf wax in vegetation and aerosols in a northern prairie ecosystem. *Oecologia, 135*, 67-77. https://doi.org/10.1007/s00442-002-1157-4

Cormier, M. -A., Werner, R. A., Sauer, P. E., Grocke, D. R., Leuenberger, M. C., Wieloch, T., et al. (2018). $^{2}$H-fractionations during the biosynthesis of carbohydrates and lipids imprint a metabolic signal on the $\delta^{2}$H values of plant organic compounds. *New Phytologist, 218*(2), 479-491. https://doi.org/10.1111/nph.15016

Cranwell, P. A., Eglinton, G., & Robinson, N. (1987). Lipid of aquatic organisms as potential contributors to lacustrine sediments II. *Organic Geochemistry*, *11*(6), 513-527. https://doi.org/10.1016/0146-6380(87)90007-6

Daniels, W. C., Russell, J. M., Giblin, A. E., Welker, J. M., Klein, E. S., & Huang, Y. (2017). Hydrogen isotope fractionation in leaf waxes in the Alaskan Arctic tundra. *Geochimica et Cosmochimica Acta*, *213*, 216-236. https://doi.org/10.1016/j.gca.2017.06.028

Dansgaard, W. (1964). Stable isotopes in precipitation. Tellus, 16, 436-469. https://doi.org/10.1111/j.2153-3490.1964.tb00181.x

DeLong, K. L., Quinn, T. M., Taylor, F. W., Lin, K., & Shen, C. -C. (2012). Sea surface temperature variability in the southwest tropical Pacific since 1649. *Nature Climate Change*, *2*, 799-804. https://doi.org/10.1038/NCLIMATE1583

Dion-Kirschner, H., McFarlin, J. M., Masterson, A. L., Axford, Y., & Osburn, M. R. (2020). Modern constraints on the sources and climate signals recorded by sedimentary plant waxes in west Greenland. *Geochemica et Cosmochimica Acta*, *286*, 336-354. https://doi.org/10.1016/j.gca.2020.07.027

Douglas, P. M. J., Pagani, M., Brenner, M., Hodell, D. A., & Curtis, J. H. (2012). Aridity and vegetation composition are important determinants of leaf-wax δD values in southeastern Mexico and Central America. *Geochimica et Cosmochimica Acta*, *97*, 24-45. https://doi.org/10.1016/j.gca.2012.09.005

Eley, Y., Dawson, L., Black, S., Andrews, J., & Pendentchouk, N. (2014). Understanding $^{2}$H/$^{1}$H systematics of leaf wax *n*-alkanes in coastal plants at Stiffkey saltmarsh, Norfolk, UK. *Geochimica et Cosmochimica Acta, 128*, 13-28. https://doi.org/10.1016/j.gca.2013.11.045

Feakins, S. J., & Sessions, A. L. (2010). Controls on the D/H ratios of plant leaf waxes in an arid ecosystem. *Geochimica et Cosmochimica Acta*, *74*(7), 2128-2141. https://doi.org/10.1016/j.gca.2010.01.016

Feng, X., D'Andrea, W. J., Zhao, C., Xin, S., Zhang, C., & Liu, W. (2019). Evaluation of leaf wax δD and soil brGDGTs as tools for paleoaltimetry on the southeastern Tibetan Plateau. *Chemical Geology*, *523*, 95-106. https://doi.org/10.1016/j.chemgeo.2019.05.005

Ficken, K. J., Li, B., Swain, D. L., & Eglinton, G. (2000). An *n*-alkane proxy for the sedimentary input of submerged/floating freshwater aquatic macrophytes. *Organic Geochemistry, 31*(7-8), 745-749. https://doi.org/10.1016/S0146-6380(00)00081-4

Freimuth, E. J., Diefendorf, A. F., & Lowell, T. V. (2017). Hydrogen isotopes of *n*-alkanes and *n*-alkanoic acids as tracers of precipitation in a temperate forest and implications for paleorecords. *Geochimica et Cosmochimica Acta, 206*, 166-183. https://doi.org/10.1016/j.gca.2017.02.027

Freimuth, E. J., Diefendorf, A. F., Lowell, T. V., Bates, B. R., Schartman, A., Bird, B. W., et al. (2020). Contrasting sensitivity of lake sediment *n*-alkanoic acids and *n*-alkanes to basin-scale vegetation and regional-scale precipitation δ2H in the Adirondack Mountains, NY (USA). *Geochimica et Cosmochimica Acta, 268*, 22-41. https://doi.org/10.1016/j.gca.2019.08.026

Freimuth, E. J., Diefendorf, A. F., Lowell, T. V., & Wiles, G. C. (2019). Sedimentary n-alkanes and n-alkanoic acids in a temperate bog are biased toward woody plants. *Organic Geochemistry*, *128*, 94-107 https://doi.org/10.1016/j.orggeochem.2019.01.006

Gamarra, B., & Kahmen, A. (2015). Concentrations and $\delta^2H$ values of cuticular *n*-alkanes vary significantly among plant organs, species and habitats in grasses from an alpine and a temperate European grassland. *Oecologia, 178*, 981-998. https://doi.org/10.1007/s00442-015-3278-6

Gao L., Edwards E. J., Zeng Y., & Huang Y. (2014). Major Evolutionary Trends in Hydrogen Isotope Fractionation of Vascular Plant Leaf Waxes. *PLoS ONE*, *9*(11): e112610. https://doi.org/10.1371/journal.pone.0112610

Gao, L., Hou, J., Toney, J., MacDonald, D., & Huang, Y. (2011). Mathematical modeling of the aquatic macrophyte inputs of mid-chain *n*-alkyl lipids to lake sediments: implications for interpreting compound specific hydrogen isotopic records. *Geochimica et Cosmochimica Acta, 75*(13), 3781-3791. https://doi.org/10.1016/j.gca.2011.04.008

Garcin, Y., Schwab, V. F., Gleixner, G., Kahmen, A., Todou, G., Sene, O., et al. (2012). Hydrogen isotope ratios of lacustrine sedimentary n-alkanes as proxies of tropical African hydrology: insights from a calibration transect across Cameroon. *Geochimica et Cosmochimica Acta, 79*, 106-126. https://doi.org/10.1016/j.gca.2011.11.039

Gillespie, T. W., Keppel, G., Pau, S., Price, J. P., Jaffre, T., & O'Neill, K. (2013). Scaling species richness and endemism of tropical dry forests on oceanic islands. *Diversity and Distributions, 19*(8), 896-906. https://doi.org/10.1111/ddi.12036

Goldsmith, Y., Polissar, P. J., deMenocal, P. B., & Broecker, W. S. (2019). Leaf wax δD and $\delta^{13}C$ in soils record hydrological and environmental information across a climatic gradient in Israel. *Journal of Geophysical Research: Biogeosciences, 124*, 2898-2916. https://doi.org/10.1029/2019JG005149

Gosling, W. D., Sear, D. A., Hassall, J. D., Langdon, P. G., Bönnen, M. N. T., Driessen, T. D., & McMichael, C. N. H. (2020). Human occupation and ecosystem change on Upolu (Samoa) during the Holocene. *Journal of Biogeography*, *47*(3), 600-614. https://doi.org/10.1111/jbi.13783

Hassall, J. D. (2017). Static or dynamic: Reconstructing past movement of the South Pacific Convergence Zone. University of Southampton.

He, D., Ladd, S. N., Sachs, J. P., & Jaffé, R. (2017). Inverse relationship between salinity and $^2H/^1H$ fractionation in leaf wax n-alkanes from Florida mangroves. *Organic Geochemistry, 110*, 1-12. https://doi.org/10.1016/j.orggeochem.2017.04.007

He, D., Ladd, S. N., Saunders, C. J., Mead, R. N., & Jaffé, R. (2020). Distribution of *n*-alkanes and their $\delta^2H$ and $\delta^{13}C$ values in typical plants along a terrestrial-coastal-oceanic gradient. *Geochimica et Cosmochimica Acta, 281*, 31-52. https://doi.org/10.1016/j.gca.2020.05.003

Hendy, E. J., Gagan, M. K., Alibert, C. A., McCulloch, M. T., Lough, J. M., & Isdale, P. J. (2002). Abrupt decrease in tropical Pacific sea surface salinity at end of Little Ice Age. *Science, 295*(5559), 1511-1514. https://doi.org/10.1126/science.1067693

Heinzelmann, S. M., Villanueva, L., Lipsewers, Y. A., Sinke-Schoen, D., Sinninghe Damsté, J. S., Schouten, S., & van der Meer, M. T. J. (2018). Assessing the metabolism of sedimentary microbial communities using the hydrogen isotope composition of fatty acids. *Organic Geochemistry, 124*, 123-132. https://doi.org/10.1016/j.orggeochem.2018.07.011

Heinzelmann S. M., Villanueva L., Sinke-Schoen D., Sinninghe Damsté J. S., Schouten S., & van der Meer M. T. J. (2015). Impact of metabolism and growth phase on the hydrogen

isotopic composition of microbial fatty acids. *Frontiers in Microbiology, 6*, 408. https://doi.org/10.3389/fmicb.2015.00408

Higley, M. C., Conroy, J. L., & Schmitt, S. (2018). Last Millennium Meridional Shifts in Hydroclimate in the Central Tropical Pacific. *Paleoceanography and Paleoclimatology, 33*(4), 354-366. https://doi.org/10.1002/2017PA003233

Hope, G. S., & Pask, J. (1998). Tropical vegetational change in the late Pleistocene of New Caledonia. *Palaeogeography, Palaeoclimatology, Palaeoecology*, *142*(1-2), 1-21. https://doi.org/10.1016/S0031-0182(97)00140-5

Hou, J., D'Andrea, W., & Huang, Y. (2008). Can sedimentary leaf waxes record D/H ratios of continental precipitation? Field, model and experimental assessments. *Geochimica et Cosmochimica Acta, 72*(14), 3503-3517. https://doi.org/10.1016/j.gca.2008.04.030

Huang, Y., Shuman, B., Wang, Y., & Webb III, T. (2004). Hydrogen isotope ratios of individual lipids in lake sediments as novel tracers of climatic and environmental change: a surface sediment test. *Journal of Paleolimnology*, *31*, 363-375. https://doi.org/10.1023/B:JOPL.0000021855.80535.13

IAEA/WMO (2015). Global Network of Isotopes in Precipitation. The GNIP Database. Accessible at: https://nucleus.iaea.org/wiser.

Jia, G., Wei, K., Chen, F., & Peng, P. (2008). Soil *n*-alkane δD vs. altitude gradients along Moung Gongga, China. *Geochimica et Cosmochimica Acta, 72*(21), 5165-5174. https://doi.org/10.1016/j.gca.2008.08.004

Kahmen, A., Hoffmann, B., Schefuss, E., Arndt, S. K., Cernusak, L. A., West, J. B., & Sachse, D. (2013). Leaf water deuterium enrichment shapes leaf wax n-alkane δD values of angiosperm plants II: Observational evidence and global implications. *Geochimica et Cosmochimica Acta, 111*, 50–63. https://doi.org/10.1016/j.gca.2012.09.004

Konecky, B. L., Noone, D. C., & Cobb, K. M. (2019). The influence of competing hydroclimate processes on stable isotope ratios in tropical rainfall. Geophysical Research Letters 46(3), 1622-1633. https://doi.org/10.1029/2018GL080188

Konecky, B. L., Russell, J., & Bijaksana, S. (2016). Glacial aridity in central Indonesia coeval with intensified monsoon circulation. *Earth and Planetary Science Letters 437*, 15-24. https://doi.org/10.1016/j.epsl.2015.12.037

Krentscher, C., Dubois, N., Camperio, G., Prebble, M., Ladd, S.N., 2019. Palmitone as a potential species-specific biomarker for the crop plant taro (*Colocasia esculenta Schott*) on remote Pacific islands. *Organic Geochemistry, 132*, 1-10. https://doi.org/10.1016/j.orggeochem.2019.03.006

Kurita, N., Ichiyanagi, K., Matsumoto, J., Yamanaka, M. D., & Ohata, T. (2009). The relationship between the isotopic content of precipitation and the precipitation amount in tropical regions. *Journal of Geochemical Exploration, 102*(3), 113-122. https://doi.org/10.1016/j.gexplo.2009.03.002

Ladd S. N., & Sachs J. P. (2012). Inverse relationship between salinity and n-alkane δD values in the mangrove *Avicennia marina*. *Organic Geochemistry, 48*, 25–36. https://doi.org/10.1016/j.orggeochem.2012.04.009

Ladd, S. N., & Sachs, J. P. (2015). Influence of salinity on hydrogen isotope fractionation in *Rhizophora* mangroves from Micronesia. *Geochimica et Cosmochimica Acta, 168*, 206–221. https://doi.org/10.1016/j.gca.2015.07.004

Ladd, S. N., & Sachs, J. P. (2017). $^{2}H/^{1}H$ fractionation in lipids of the mangrove *Bruguiera gymnorhiza* increases with salinity in marine lakes of Palau. *Geochimica et Cosmochimica Acta, 204*, 300-312. https://doi.org/10.1016/j.gca.2017.01.046

Ladd, S. N., Nelson, D. B., Schubert, C. J., & Dubois, N. (2018). Lipid compound classes display diverging hydrogen isotope responses in lakes along a nutrient gradient. *Geochimica et Cosmochimica Acta, 237*, 103-119. https://doi.org/10.1016/j.gca.2018.06.005

Lee, H., Feakins, S. J., Lu, Z., Schimmelmann, A., Sessions, A. L., Tierney, J. E., Williams, T. J. (2017). Comparison of three methods for the methylation of aliphatic and aromatic compounds. *Rapid Communications in Mass Spectrometry, 31*, 1633-1640. https://doi.org/10.1002/rcm.7947

Leider, A., Hinrichs, K. -U., Schefuss, E., & Versteegh, G. J. M. (2013). Distribution and stable isotopes of plant wax derived n-alkanes in lacustrine, fluvial and marine surface sediments along an Eastern Italian transect and their potential to reconstruct the hydrological cycle. *Geochimica et Cosmochimica Acta, 117*, 16-32. https://doi.org/10.1016/j.gca.2013.04.018

Li C., Sessions A. L., Kinnaman F. S., & Valentine D. L. (2009). Hydrogen-isotopic variability in lipids from Santa Barbara Basin sediments. *Geochimica et Cosmochimica Acta, 73*, 4803-4823. https://doi.org/10.1016/j.gca.2009.05.056

Li, Y., Yang, S., Luo, P., & Xiong, S. (2019). Aridity-controlled hydrogen isotope fractionation between soil *n*-alkanes and precipitation in China. *Organic Geochemistry, 133*, 53-64. https://doi.org/10.1016/j.orggeochem.2019.04.009

Linsley, B. K., Kaplan, A., Gouriou, Y., Salinger, J., DeMenocal, P., Wellington, G. M., & Howe, S. S. (2006). Tracking the extent of the South Pacific Convergence Zone since the early 1600s. *Geochemistry, Geophysics, and Geosystems, 7*, 1-15. https://doi.org/10.1029/2005GC001115

Linsley, B. K., Wellington, G. M., Schrag, D. P., Ren, L., Salinger, M. J., & Tudhope, A. W. (2004). Geochemical evidence from corals for changes in the amplitude and spatial pattern of South Pacific interdecadal climate variability over the last 300 years. *Climate Dynamics, 22*, 1-11. https://doi.org/10.1007/s00382-003-0364-y

Liu, J., & An, Z. (2019). Variations in hydrogen isotope fractionation in higher plants and sediments across different latitudes: Implications for paleohydrological reconstruction. *Science of the Total Environment, 650*(1), 470-478. https://doi.org/10.1016/j.scitotenv.2018.09.047

Lu, J., Zang, J., Meyers, P., Huang, X., Qiu, P., Yu, X., et al. (2020). Surface soil *n*-alkane molecular and δD distributions along a precipitation transect in northeastern China. *Organic Geochemicstry 144*, 104015. https://doi.org/10.1016/j.orggeochem.2020.104015

Maloney, A. E., Nelson, D. B., Richey, J. N., Prebble, M., Sear, D. A., Hassell, J. D., et al. (2019). Reconstructing precipitation in the tropical South Pacific from dinosterol $^{2}H/^{1}H$ ratios in lake sediment. *Geochimica et Cosmochimica Acta, 245*, 190-206. https://doi.org/10.1016/j.gca.2018.10.028

Maupin, C. R., Partin, J. W., Shen, C. -C., Quinn, T. M., Lin, K., Taylor, F. W., et al. (2014). Persistent decadal-scale rainfall variability in the tropical South Pacific Convergence Zone through the past six centuries. *Climate of the Past 10*, 1319-1332. https://doi.org/10.5194/cp-10-1319-2014

McFarlin, J. M., Axford, Y., Masterson, A. L., & Osburn, M. R. (2019). Calibration of modern sedimentary $\delta^{2}H$ plant wax-water relationships in Greenland lakes. *Quaternary Science Reviews, 225*, 105978. https://doi.org/10.1016/j.quascirev.2019.105978

Meyers, P. A. (2003). Applications of organic geochemistry to paleolimnological reconstructions: a summary of examples from the Laurentian Great Lakes. *Organic Geochemistry, 34*(2), 261-289. https://doi.org/10.1016/S0146-6380(02)00168-7

Moore, P. D., Webb, J. A., & Collinson, M. E. (1991). Pollen analysis. Blackwell Scientific, Oxford.

Mueller-Dombois, D., & Fosberg, F. R. (1998). Vegetation of the tropical Pacific islands. Springer, New York.

Nelson, D. B., (2013). Hydrogen isotopes from lipid biomarkers: Purification, field calibration, and application to reconstructing Galapagos paleohyrology. University of Washington.

Nelson D. B., & Sachs J. P. (2016). Galápagos hydroclimate of the Common Era from paired microalgal and mangrove biomarker $^{2}H/^{1}H$ values. *Proceedings of the National Academy of Sciences of the United States of America, 113*(13), 3476-3481. https://doi.org/10.1073/pnas.1516271113

Nelson, D. B., Knohl, A., Sachse, D., Schefuß, E., & Kahmen, A. (2017). Sources and abundances of leaf waxes in aerosols in central Europe. *Geochimica et Cosmochimica Acta, 198*, 299-314. https://doi.org/10.1016/j.gca.2016.11.018

Nelson, D. B., Ladd, S. N., Schubert, C. J., & Kahmen, A. (2018). Rapid atmospheric transport and large-scale deposition of recently synthesized plant waxes. *Geochimica et Cosmochimica Acta, 222*, 599-617. https://doi.org/10.1016/j.gca.2017.11.018

Newberry, S. L., Kahmen, A., Dennis, P., & Grant, A. (2015). *n*-Alkane biosynthetic hydrogen isotope fractionation is not constant throughout the growing season in the riparian tree *Salix viminalis*. *Geochimica et Cosmochimica Acta, 165*, 75-85. https://doi.org/10.1016/j.gca.2015.05.001

Newberry, S. L., Nelson, D. B., & Kahmen, A. (2017). Cryogenic vacuum artifacts do not affect plant water-uptake studies using stable isotope analysis. *Ecohydrology* 10:e1892. https://doi.org/10.1002/eco.1892

Osburn, M. R., Sessions, A. L., Pepe-Ranney, C., Spear, J. R. (2011). Hydrogen-isotopic variability in fatty acids from Yellowstone National Park hot spring microbial communities. *Geochimica et Cosmochimica Acta, 75*(17), 4830-4845. https://doi.org/10.1016/j.gca.2011.05.038

Partin, J. W., Quinn, T. M., Shen, C. -C., Emile-Geay, J., Taylor, F. W., Maupin, C. R., et al. (2013). Multidecadal rainfall variability in South Pacific Convergence Zone as revealed by stalagmite geochemistry. *Geology, 41*(11), 1143-1146. https://doi.org/10.1130/G34718.1

Peterse, F., van der Meer, M. T. J., Schouten, S., Jia, G., Ossebaar, J., Blokker, J., & Sinninghe Damste, J. S. (2009). Assessment of soil *n*-alkane δD and branched tetraether membrane lipid distributions as tools for paleoelevation reconstruction. *Biogeosciences, 6*, 2799-2807.

Prebble, M., & Wilmshurst, J.M. (2009). Detecting the initial impact of humans and introduced species on island environments in Remote Oceania using palaeoecology. *Biological Invasions, 11*, 1529–1556. https://doi.org/10.1007/s10530-008-9405-0

Prebble, M., Anderson, A. J., Augustinus, P., Emmitt, J., Fallon, S. J., Furey, L. L., et al. (2019). Early tropical Pacific production in marginal subtropical and temperate Polynesia. *Proceedings of the National Academy of Sciences of the United States of America 116*(18), 8824-8833. https://doi.org/10.1073/pnas.1821732116

Polissar, P. J., & Freeman, K. H. (2010). Effects of aridity and vegetation on plant-wax δD in modern lake sediments. *Geochimica et Cosmochimica Acta, 74*(20), 5785-5797. https://doi.org/10.1016/j.gca.2010.06.018

Quinn, T. M., Crowley, T. J., Taylor, F. W., & Henin, C. (1998). A multicentury stable isotope record from a New Caledonia coral: interannual and decadal sea surface temperature variability in the Southwest Pacific since 1657 AD. *Paleoceanography, 13*(4), 412-426. https://doi.org/10.1029/98PA00401

Quinn, T. M., Taylor, F. W., & Crowley, T. J. (1993). A 173 year stable isotope record from a tropical South Pacific coral. *Quaternary Science Reviews, 12*(6), 407-418. https://doi.org/10.1016/S0277-3791(05)80005-8

Reef R., Markham H. L., Santini N. S., & Lovelock C. E., (2015). The response of the mangrove *Avicennia marina* to heterogeneous salinity measured using a split-root approach. *Plant Soil, 393*, 297–305. https://doi.org/ 10.1007/s11104-015-2489-2

Richey, J. N., & Sachs, J. P. (2016). Precipitation changes in the western tropical Pacific over the past millennium. *Geology, 44*(8), 671-674. https://doi.org/10.1130/G37822.1

Rozanski, K., Araguas-Araguas, L, & Gonfiantinin, R. (1993). Isotopic patterns in modern global precipitation. In P. K. Swart (Ed.) *Climate Change in Continental Isotopic Records, Volume 78* (pp. 1-36). Washington, DC: American Geophysical Union. https://doi.org/10.1029/GM078p0001

Sachs, J. P., Blois, J. L., McGee, T., Wolhowe, M., Haberle, S., Clark, G., Atahan, P. (2018). Southward shift of the Pacific ITCZ during the Holocene. *Paleoceanography and Paleoclimatology, 33*(12), 1383-1395. https://doi.org/10.1029/2018PA003469

Sachs J. P., Sachse D., Smittenberg R. H., Zhang Z., Battisti D. S., & Golubic S. (2009). Southward movement of the Pacific intertropical convergence zone AD 1400–1850. *Nature Geoscience, 2*, 519–525. https://doi.org/10.1038/NGEO554

Sachse, D., Billault, I., Bowen, G. J., Chikaraishi, Y., Dawson, T. E., Feakins, S. J., et al. (2012). Molecular Paleohydrology: Interpreting the hydrogen-isotopic composition of lipid biomarkers from photosynthesizing organisms. *Annual Review of Earth and Planetary Sciences, 40*, 221–249. https://doi.org/10.1146/annurev-earth-042711-105535

Sachse D., Radke J., & Gleixner G. (2004). Hydrogen isotope ratios of recent lacustrine sedimentary n-alkanes record modern climate variability. *Geochimica et Cosmochimica Acta, 68*(23), 4877-4889. https://doi.org/10.1016/j.gca.2004.06.004

Santini N. S., Reef R., Lockington D. A., & Lovelock C. E. (2015). The use of fresh and saline water sources by the mangrove Avicennia marina. *Hydrobiologia, 745*, 59–68. https://doi.org/10.1007/s10750-014-2091-2

Scholl, M. A., Giambelluca, T. W., Gingerich, S. B., Nullet, M. A., Loope, L. L. (2007). Cloud water in windward and leeward mountain forests: The stable isotope signature of orographic cloud water. *Water Resources Research, 43*, W12411. https://doi.org/10.1029/2007WR006011

Scholl, M. A., Ingebritsen, S. E., Janik, C. J., Kauahikaua, J. P. (1996). Use of precipitation and groundwater isotopes to interpret region hydrology on a tropical volcanic island: Kilauea volcano area, Hawaii. *Water Resources Research, 32*, 3525-3537. https://doi.org/10.1029/95WR02837

Schwab, V. F., Garcin, Y., Sachse, D., Todou, G., Sene, O., Onana, J. M., et al. (2015). Effect of aridity on $\delta^{13}C$ and $\delta D$ values of C3 plant- and C4 graminoid-derived leaf wax lipids from soils along an environmental gradient in Cameroon (Western Central Africa). *Organic Geochemistry, 78*, 99-109. https://doi.org/10.1016/j.orggeochem.2014.09.007

Sear, D. A., Allen, M. S., Hassall, J. D., Maloney, A. E., Langdon, P. G., Morrison, A. E., et al. (2020). Human settlement of East Polynesia earlier, incremental, and coincident with prolonged South Pacific drought. *Proceedings of the National Academy of Sciences of the United States of America, 117*(16), 8813-8819. https://doi.org/10.1073/pnas.1920975117.

Sharmila, S., & Walsh, K. J. E. (2018). Recent poleward shift of tropical cyclone formation linked to Hadley cell expansion. *Nature Climate Change, 8*, 730-736. https://doi.org/10.1038/s41558-018-0227-5

Sichrowsky, U., Schabetsberger, R., Sonntag, B., Stoyneva, M., Maloney, A. E., Nelson, D. B., et al. (2014). Limnological characterization of volcanic crater lakes on Uvea Island (Wallis and Futuna, South Pacific). *Pacific Science, 68*(3), 333-343. https://doi.org/10.2984/68.3.3

Smittenberg R. H., Saenger C., Dawson M. N., & Sachs J. P. (2011). Compound-specific D/H ratios of the marine lakes of Palau as proxies for West Pacific Warm Pool hydrologic variability. *Quaternary Science Reviews, 30*(7-8), 921-933. https://doi.org/10.1016/j.quascirev.2011.01.012

Southern, W. (1986). The Late Quaternary Environmental History of Fiji. Australian National University.

Steen-Larsen, H. C., Risi, C., Werner, M., Yoshimura, K., Masson-Delmotte, V. (2017). Evaluating the skills of isotope-enabled general circulation models against in situ atmospheric water vapor isotope observations. *JGR Atmospheres, 122*(1), 246-263. https://doi.org/10.1002/2016JD025443

Stevenson, J., Dodson, J. R., & Prosser, I. P. (2001). A late Quaternary record of environmental change and human impact from New Caledonia. *Palaeogeography, Palaeoclimatology, Palaeoecology, 168*(1-2), 97–123. https://doi.org/10.1016/S0031-0182(00)00251-0

Struck, J., Bliedtner, M., Strobel, P., Bittner, L., Bazarradnaa, E., Andreeva, D., et al. (2020). Leaf waxes and hemicelluloses in topsoils reflect the d2H anv d18O isotopic composition of precipitation in Mongolia. Frontiers in Earth Science. 8:343. https://doi.org/10.3389/feart.2020.00343

Sturm, C., Zhang, Q., & Noone, D. (2010). An introduction to stable water isotopes in climate models: Benefits of forward proxy modeling for paleoclimatology. *Climate of the Past, 6*, 115-129. https://doi.org/10.5194/cpd-5-1697-2009

Tan, J., Jakob, C., Rossow, W. B., & Tselioudis, G. (2015). Increases in tropical rainfall driven by changes in frequency of organized deep convection. *Nature. 519*, 451-454. https://doi.org/10.1038/nature14339

Terry, J. P. (2011). The Climate of Santo (Vanuatu). In P. Bouchet, H. Le Guyander, O. Pascal (Eds.), *The Natural History of Santo* (pp. 52-56). Paris, France: Museum National d'Histoire Naturelle.

Tierney, J. E., deMenocal, P. B., & Zander, P. D. (2017). A climatic context for the out-of-Africa migration. *Geology*, 45 (11): 1023–1026. https://doi.org/10.1130/G39457.1

Tipple B. J., Berke M. A., Doman C. E., Khachaturyan S., & Ehleringer J. R. (2013). Leaf *n*-alkanes record the plant-water environment at leaf flush. *Proceedings of the National Academy of Sciences of the United States of America 110*(7), 2659–2664. https://doi.org/10.1073/pnas.1213875110

Tipple, B. J., Berke M. A., Hambach B., Roden J. S., & Ehleringer J. R. (2015). Predicting leaf wax *n*-alkane $^{2}H/^{1}H$ ratios: Controlled water source and humidity experiments with hydroponically grown trees confirm predictions of Craig-Gordon model. *Plant, Cell and Environment, 38*(6), 1035-1047. https://doi.org/10.1111/pce.12457

van Bree, L. G. J., Peterse, F., van der Meer, M. T. J., Middelburg, J. J., Negash, A. M. D., De Crop, W., et al. (2018). Seasonal variability in the abundance and stable carbon-isotopic composition of lipid biomarkers in suspended particulate matter from a stratified equatiorial lake (Lake Chala, Kenya/Tanzania): Implications for the sedimentary record. *Quaternary Science Reviews, 192*, 208-224. https://doi.org/10.1016/j.quascirev.2018.05.023

van der Veen, I., Peterse, F., Davenport, J., Meese, B., Bookhagen, B., France-Lanord, C., et al. (2020). Validation and calibration of soil $\delta^{2}H$ and brGDGTs along (E-W) and strike (N-S)

of the Himalayan climatic gradient. *Geochimica et Cosmochimica Acta*. https://doi.org/10.1016/j.gca.2020.09.014

Volkman J. K. (2003). Sterols in microorganisms. *Applied Microbiology and Biotechnology*, *60*, 495–506. https://doi.org/10.1007/s00253-002-1172-8

Volkman J. K., Johns R. B., Gillian, F. T., & Perry G. J. (1980). Microbial lipids of an intertidal sediment – I. Fatty acids and hydrocarbons. *Geochimica et Cosmochimica Acta*, *44*(8), 1133-1143. https://doi.org/10.1016/0016-7037(80)90067-8

Wu, M. S., West, A. J., & Feakins, S. J. (2019). Tropical soil profiles reveal the fate of plant wax biomarkers during soil storage. *Organic Geochemistry*, *128*, 1-15. https://doi.org/10.1016/j.orggeochem.2018.12.011

Yoshimura, K., Kanamitsu, M., Noone, D., & Oki, T. (2018). Historical isotope simulation using reanalysis atmospheric data. *Journal of Geophysical Research: Atmospheres*, *113*(D19), D19108. https://doi.org/10.1029/2008JD010074

Zhang X., Gillespie A., & Sessions A. L. (2009). Large D/H variations in bacterial lipids reflect central metabolic pathways. *Proceedings of the National Academy of Sciences of the United States of America*, *106*(31), 12580-12586. https://doi.org/10.1073/pnas.0903030106

Zhang Z., & Sachs J. P. (2007). Hydrogen isotope fractionation in freshwater algae: 1. Variations among lipids and species. *Organic Geochemistry*, *38*(4), 582–608. https://doi.org/10.1016/j.orggeochem.2006.12.004

**Table 1** Lake location, total number of samples analyzed per site, $\delta^2H$ values of local precipitation and leaf waxes, and measured $\delta^2H_{Wax}$ values with residuals from predicted values based on linear correlation of compiled literature values

| Site, Island, Country | Lat. (°N)[1] | Long. (°E)[1] | # of samples | $\delta^2H_P$ (‰, VSMOW)[2] | $\delta^2H$ *n*–$C_{29}$ alkane[3] (residual from global relationship[4]) (‰, VSMOW) | $\delta^2H$ *n*–$C_{28}$ acid[3] (residual from global relationship[4]) (‰, VSMOW) |
|---|---|---|---|---|---|---|
| **Lakes** | | | | | | |
| Rimatu'u Pond, Tetiaroa, French Polynesia | −17.0249 | 210.4417 | 2 | −25 ± 26 | −177 (–38 ± 12) | −160 ± 17 (–28 ± 19) |
| Oroatera Pond, Tetiaroa, French Polynesia | −16.9958 | 210.4591 | 1 | −25 ± 26 | −173 (–34 ± 12) | *N.A.* |
| Onetahi Pond, Tetiaroa, French Polynesia[#] | −17.0207 | 210.4081 | 1 | −25 ± 26 | −139 (–0 ± 12) | −126 (5 ± 10) |
| Lake Lanoto'o, Upolu, Samoa | −13.9109 | 188.1726 | 3 | −34 ± 3 | −159 (–12 ± 1) | −148 ± 6 (–9 ± 6) |
| Lac Lalolalo, Wallis, Wallis and Futuna | −13.3017 | 183.7662 | 3 | −23 ± 1 | *N.A.* | −150 ± 6 (–20 ± 6) |
| Lac Lanutavake, Wallis, Wallis and Futuna | −13.3212 | 183.7860 | 2 | −24 ± 2 | *N.A.* | −140 ± 9 (–9 ± 9) |
| Lake Dranoniveilomo, Vanua Balavu, Fiji | −17.1976 | 181.0441 | 2 | −21 ± 11 | −151 (–15 ± 5) | −173 ± 14 (–44 ± 14) |
| Lake Tagamaucia, Teveuni, Fiji[#] | −16.8163 | 180.0601 | 2 | −34 ± 14 | −170 ± 1 (–23 ± 7) | −175 ± 1 (–36 ± 5) |
| Otas Lake, Efate, Vanuatu | −17.6945 | 168.5850 | 1 | −34 ± 73 | −154 (–6 ± 35) | −136 (2 ± 27) |
| Emaotul Lake, Efate, Vanuatu | −17.7342 | 168.4151 | 3 | −36 ± 76 | −152 ± 9 (–3 ± 36) | −130 ± 3 (9 ± 26) |
| White Lake, Thion, Vanuatu | −15.0410 | 167.0892 | 2 | −35 ± 70 | −174 (–25 ± 34) | −119 ± 2 (21 ± 26) |
| Waérowa East Lake, Espiritu Santo, Vanuatu[#] | −15.5950 | 167.0788 | 1 | −34 ± 71 | *N.A.* | −155 (–16 ± 27) |
| Nopovois Pond, Espiritu Santo, Vanuatu | −15.4970 | 166.7357 | 1 | −40 ± 71 | −154 (–1 ± 34) | −122 (21 ± 27) |
| Vesalea Pond, Espiritu Santo, Vanuatu[#] | −15.1589 | 166.6549 | 1 | −40 ± 70 | −157 (–4 ± 34) | *N.A.* |
| Lake Hut, Grande Terre, New Caledonia | −22.2609 | 166.9526 | 2 | −15 ± 54 | −161 ± 2 (–31 ± 26) | −133 ± 1 (–8 ± 20) |
| Lake Tavara, Tetepare, Solomon Islands | −8.7029 | 157.4503 | 1 | −46 ± 43 | −162 (–4 ± 21) | −156 (–9 ± 16) |
| Lake Rano, Rendova, Solomon Islands | −8.6879 | 157.3243 | 2 | −47 ± 42 | *N.A.* | −135 ± 5 (13 ± 17) |
| Harai Lake #1, Rendova, Solomon Islands | −8.5622 | 157.3556 | 1 | −47 ± 42 | *N.A.* | −121 (27 ± 16) |
| Harai Lake #3, Rendova, Solomon Islands | −8.5648 | 157.3651 | 2 | −47 ± 42 | *N.A.* | −134 ± 11 (15 ± 19) |
| **Mangrove swamps** | | | | | | |
| Sapwalap Swamp, Pohnpei, Fed. States of Micronesia | 6.88 | 158.30 | 5 | −33 ± 2 | −150 ± 5 (–3 ± 5) | *N.M.* |
| Tol Swamp, Chuuk, Fed. States of Micronesia | 7.35 | 150.60 | 4 | −32± 1 | −153 ± 5 (–2 ± 5) | *N.M.* |
| Sasa Swamp, Guam, United States | 13.45 | 140.73 | 4 | −29 ± 1 | −145 ± 5 (–7 ± 5) | *N.M.* |
| Galal Swamp, Yap, Fed. States of Micronesia | 9.50 | 138.08 | 5 | −34 ± 1 | −151 ± 6 (–3 ± 6) | *N.M.* |

[1]Less precision is provided for latitude and longitude in mangrove swamps because swamp samples were collected along a transect typically spanning > 1 km.

[2]Mean annual precipitation $\delta^2H$ values (relative to VSMOW) from OIPC ± 95% confidence intervals.

[3]Mean value of multiple surface sediment measurements from same lake, relative to VSMOW. Uncertainties represent 1 standard deviation. When only one sample was analyzed no uncertainty is reported. Analytical uncertainty for compound specific $\delta^2H$ measurements is 4‰. *"N.A."* = compound was not present or was below detection limit for $\delta^2H$ measurements. "*N.M.*" = not measured.

[4]Residuals are offsets from global calibration line of compiled leaf wax $\delta^2H$ values from the literature. Uncertainties are site specific standard deviations of OIPC $\delta^2H$ values, and are propagated with standard deviations of leaf wax $\delta^2H$ values when multiple samples are available from a site.

[#]Lakes with greater than 50% vegetation cover

**Table 2** Pollen counts from near surface sediments, reported as a percentage of total palynmorphs counted. For each sediment sample, age ranges are presented for the top and bottom depth.

| Site, Island, Country | Depth of pollen sample (cm) | Bacon age at top of interval (year C.E.)$ | Bacon age at bottom of interval (year C.E.)$ | Primary forest (%) | Secondary forest (%) | Mangroves (%) | Ferns (%) | Non-vascular plants (%) | Dryland herbs (%) | Wetland herbs (%) | Aquatic plants (%) | Unknown (%) |
|---|---|---|---|---|---|---|---|---|---|---|---|---|
| Lake Lanoto'o, Upolu, Samoa | 1-2 | 2013 ± 1 | 2002 ± 1 | 3.0 | 24.6 | 0 | 62.8 | 0 | 2.7 | 6.9 | 0 | 0 |
| Lac Lalolalo, Wallis, Wallis and Futuna* | 1-3 | 2001 +8 -14 | 1991 + 14 -19 | 10.3 | 57.1 | 0 | 16.4 | 0 | 0.4 | 13.4 | 0.8 | 1.7 |
| Lac Lanutavake, Wallis, Wallis and Futuna | 3-4 | 1990 +20 -64 | 1983 +26 -86 | 13.1 | 69.1 | 0 | 4.3 | 0 | 6.2 | 4.6 | 0 | 2.7 |
| Lake Dranoniveilomo, Vanua Balavu, Fiji | 2-3 | 2010 ± 2 | 2009 ± 3 | 21.0 | 33.6 | 0.7 | 17.5 | 1.4 | 4.2 | 19.6 | 0 | 2.1 |
| Lake Tagamaucia, Teveuni, Fiji# | 2-3 | 1989 ± 7 | 1978 ± 10 | 5.1 | 13.4 | 0 | 58.6 | 0 | 0.6 | 21.3 | 0 | 1.0 |
| Otas Lake, Efate, Vanuatu | 2-3 | N.A. | N.A. | 4.7 | 52.1 | 15.6 | 2.7 | 0 | 0 | 21.8 | 0.8 | 2.3 |
| Emaotul Lake, Efate, Vanuatu | 1-2 | 2016 ± 3.4 | 2014 ± 3.4 | 4.9 | 55.8 | 0 | 12.7 | 0.3 | 11.4 | 8.4 | 5.2 | 1.3 |
| White Lake, Thion, Vanuatu | 3-4 | 1997 +23 -14 | 1991 +30 -19 | 1.3 | 42.3 | 0 | 39.3 | 0 | 2.1 | 11.7 | 0 | 3.4 |
| Waérowa East Lake, Espiritu Santo, Vanuatu# | 3-1 | 2010 ± 3 | 2009 ± 3 | 1.2 | 11.2 | 14.1 | 35.9 | 0 | 11.2 | 14.7 | 7.7 | 4.1 |
| Nopovois Pond, Espiritu Santo, Vanuatu | 0-1 | 2017 | N.A. | 16.3 | 53.5 | 0 | 15.0 | 0 | 8.9 | 3.1 | 0.3 | 2.6 |
| Vesalea Pond, Espiritu Santo, Vanuatu# | 0-1 | 2016 +1 -3 | 2005 +10 -14 | 6.5 | 46.2 | 0 | 18.8 | 1.5 | 11.4 | 6.8 | 4.6 | 4.3 |
| Lac Hut, Grand Terre, New Caledonia | 0-1 | N.A. | N.A. | 50.1 | 41.1 | 0 | 4.8 | 0 | 0 | 0.9 | 0 | 3.1 |
| Lake Tavara, Tetepare, Solomon Islands | 8-9 | 1996 ± 5 | 1993 ± 6 | 6.3 | 23.4 | 6.3 | 54.7 | 0 | 1.6 | 7.8 | 0 | 0.1 |
| Lake Rano, Rendova, Solomon Islands | 9-10 | 1969 +17 -16 | 1960 +21 -20 | 16.7 | 46.5 | 0 | 29.8 | 0 | 0 | 4.4 | 0.9 | 1.8 |
| Harai Lake #1, Rendova, Solomon Islands | 11-12 | 1716 +99 -123 | 1702 +103 - 120 | 5.4 | 19.4 | 2.2 | 66.7 | 0 | 0 | 5.4 | 0 | 1.1 |
| Harai Lake #3, Rendova, Solomon Islands | 30-31 | 1871 ± 85 | 1866 +86 -84 | 3.1 | 5.2 | 0 | 91.8 | 0 | 0 | 0 | 0 | 0 |

*Mean of 2 samples from different sites in these lakes. Age ranges presented represented the mean age for the top and bottom of each interval, and the full range of possible ages for both sites.

# Lakes with greater than 50% vegetation cover

$ Age ranges are provided from sites with existing age models, the details of which are provided by Maloney et al. (2019), Krentscher et al. (2019), Gosling et al. (2020), and Sear et al. (2020)

**Figure 1.**

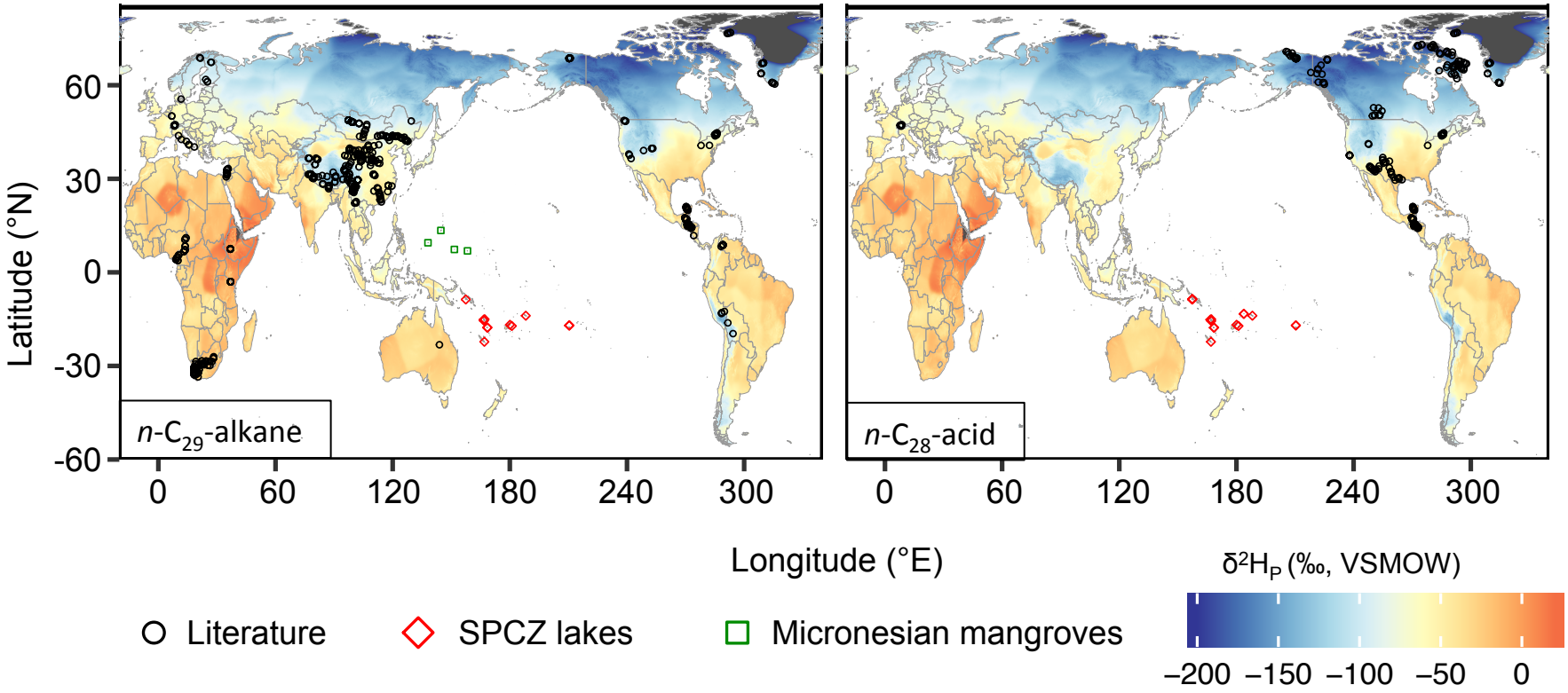
Latitude (°N)
60
30
0
-30
-60
n-C29-alkane
n-C28-acid
0
60
120
180
240
300
Longitude (°E)
δ2HP (‰, VSMOW)
–200
–150
–100
–50
0
Literature
SPCZ lakes
Micronesian mangroves

**Figure 2.**

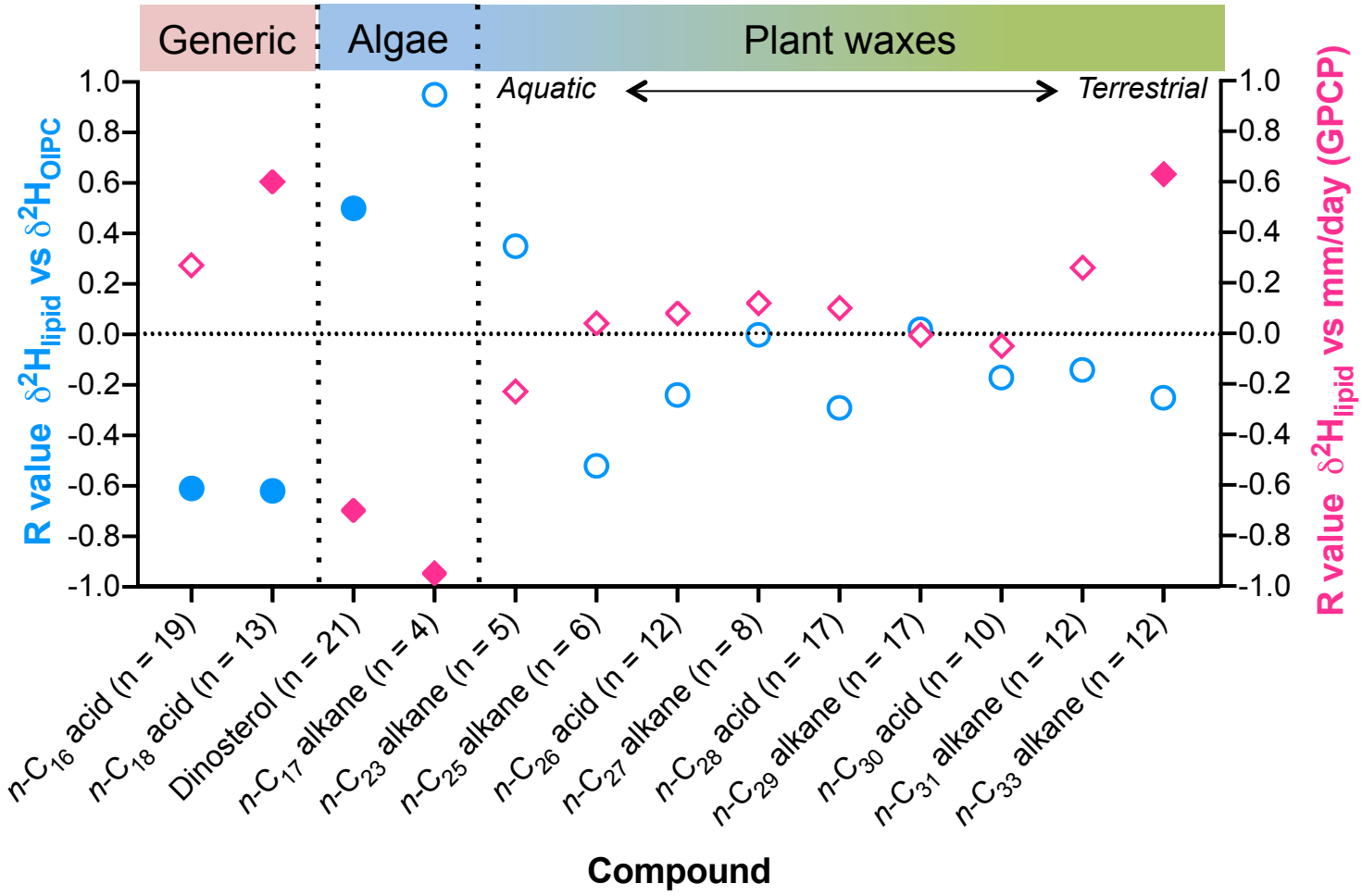
Generic
Algae
Plant waxes
Aquatic
Terrestrial
R value $\delta^2H_{lipid}$ vs $\delta^2H_{OIPC}$
R value $\delta^2H_{lipid}$ vs mm/day (GPCP)
1.0
0.8
0.6
0.4
0.2
0.0
-0.2
-0.4
-0.6
-0.8
-1.0
n-C16 acid (n = 19)
n-C18 acid (n = 13)
Dinosterol (n = 21)
n-C17 alkane (n = 4)
n-C23 alkane (n = 5)
n-C25 alkane (n = 6)
n-C26 acid (n = 12)
n-C27 alkane (n = 8)
n-C28 acid (n = 17)
n-C29 alkane (n = 17)
n-C30 acid (n = 10)
n-C31 alkane (n = 12)
n-C33 alkane (n = 12)
Compound

**Figure 3.**

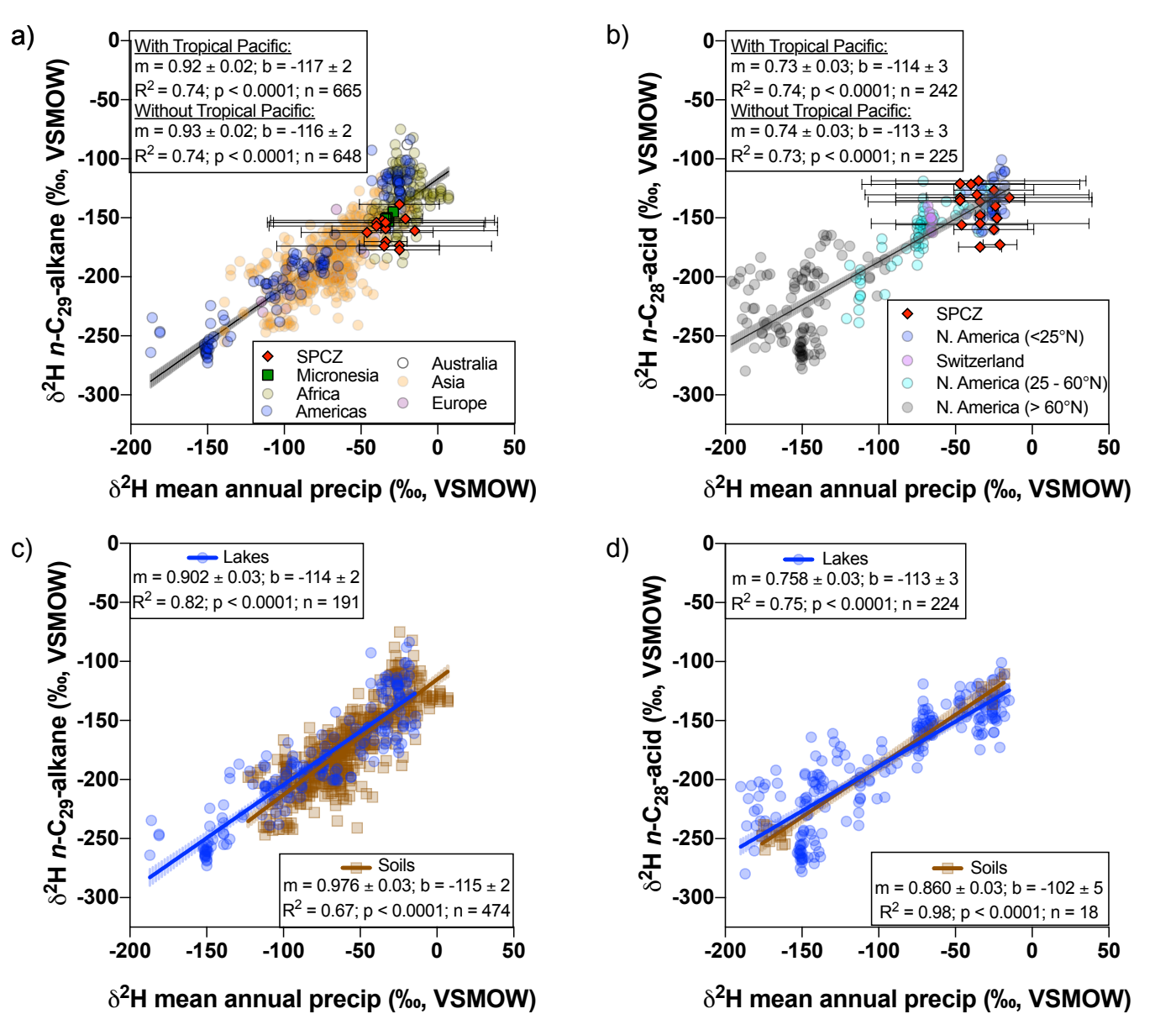
a)
With Tropical Pacific:
m = 0.92 ± 0.02; b = -117 ± 2
R2 = 0.74; p < 0.0001; n = 665
Without Tropical Pacific:
m = 0.93 ± 0.02; b = -116 ± 2
R2 = 0.74; p < 0.0001; n = 648
SPCZ
Micronesia
Africa
Americas
Australia
Asia
Europe
δ2H n-C29-alkane (‰, VSMOW)
δ2H mean annual precip (‰, VSMOW)
b)
With Tropical Pacific:
m = 0.73 ± 0.03; b = -114 ± 3
R2 = 0.74; p < 0.0001; n = 242
Without Tropical Pacific:
m = 0.74 ± 0.03; b = -113 ± 3
R2 = 0.73; p < 0.0001; n = 225
SPCZ
N. America (<25°N)
Switzerland
N. America (25 - 60°N)
N. America (> 60°N)
δ2H n-C28-acid (‰, VSMOW)
δ2H mean annual precip (‰, VSMOW)
c)
Lakes
m = 0.902 ± 0.03; b = -114 ± 2
R2 = 0.82; p < 0.0001; n = 191
Soils
m = 0.976 ± 0.03; b = -115 ± 2
R2 = 0.67; p < 0.0001; n = 474
δ2H n-C29-alkane (‰, VSMOW)
δ2H mean annual precip (‰, VSMOW)
d)
Lakes
m = 0.758 ± 0.03; b = -113 ± 3
R2 = 0.75; p < 0.0001; n = 224
Soils
m = 0.860 ± 0.03; b = -102 ± 5
R2 = 0.98; p < 0.0001; n = 18
δ2H n-C28-acid (‰, VSMOW)
δ2H mean annual precip (‰, VSMOW)

**Figure 4.**

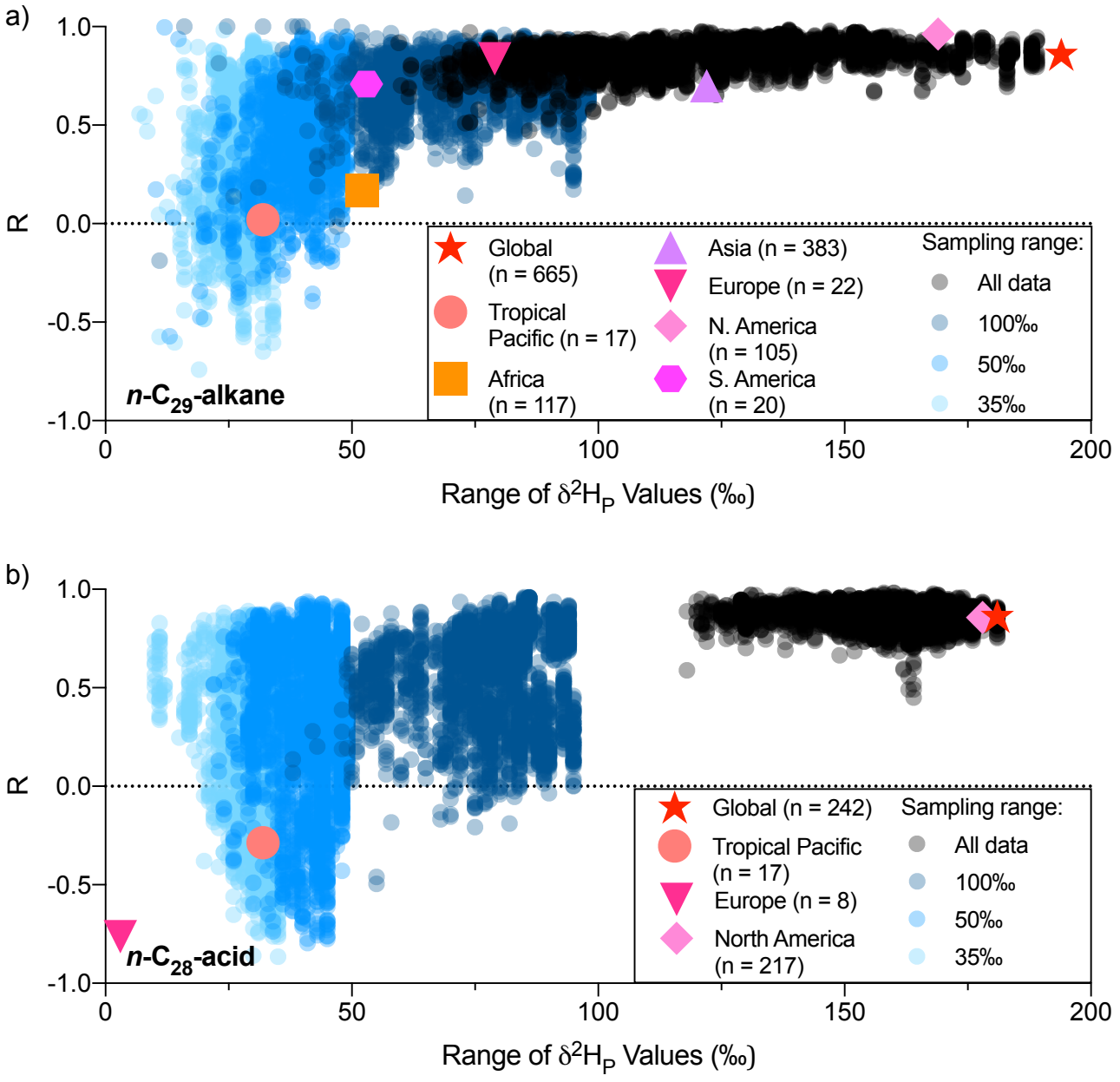
a)
1.0
0.5
0.0
-0.5
-1.0
R
0
50
100
150
200
Range of δ²H_P Values (‰)
n-C29-alkane
Global (n = 665)
Tropical Pacific (n = 17)
Africa (n = 117)
Asia (n = 383)
Europe (n = 22)
N. America (n = 105)
S. America (n = 20)
Sampling range:
All data
100‰
50‰
35‰
b)
1.0
0.5
0.0
-0.5
-1.0
R
0
50
100
150
200
Range of δ²H_P Values (‰)
n-C28-acid
Global (n = 242)
Tropical Pacific (n = 17)
Europe (n = 8)
North America (n = 217)
Sampling range:
All data
100‰
50‰
35‰

**Figure 5.**

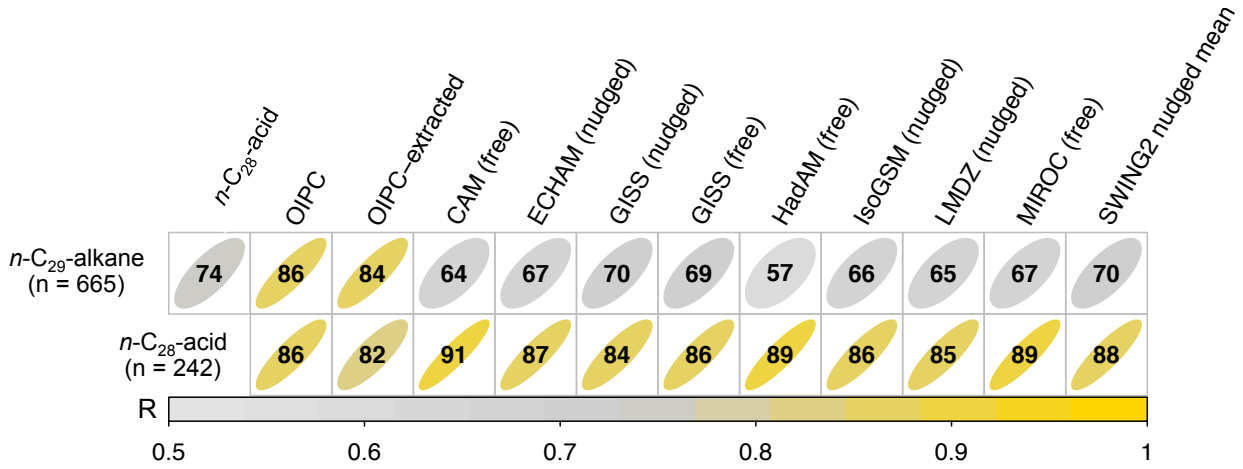
n-C28-acid
OIPC
OIPC–extracted
CAM (free)
ECHAM (nudged)
GISS (nudged)
GISS (free)
HadAM (free)
IsoGSM (nudged)
LMDZ (nudged)
MIROC (free)
SWING2 nudged mean
n-C29-alkane (n = 665)
74 86 84 64 67 70 69 57 66 65 67 70
n-C28-acid (n = 242)
86 82 91 87 84 86 89 86 85 89 88
R
0.5 0.6 0.7 0.8 0.9 1

**Figure 6.**

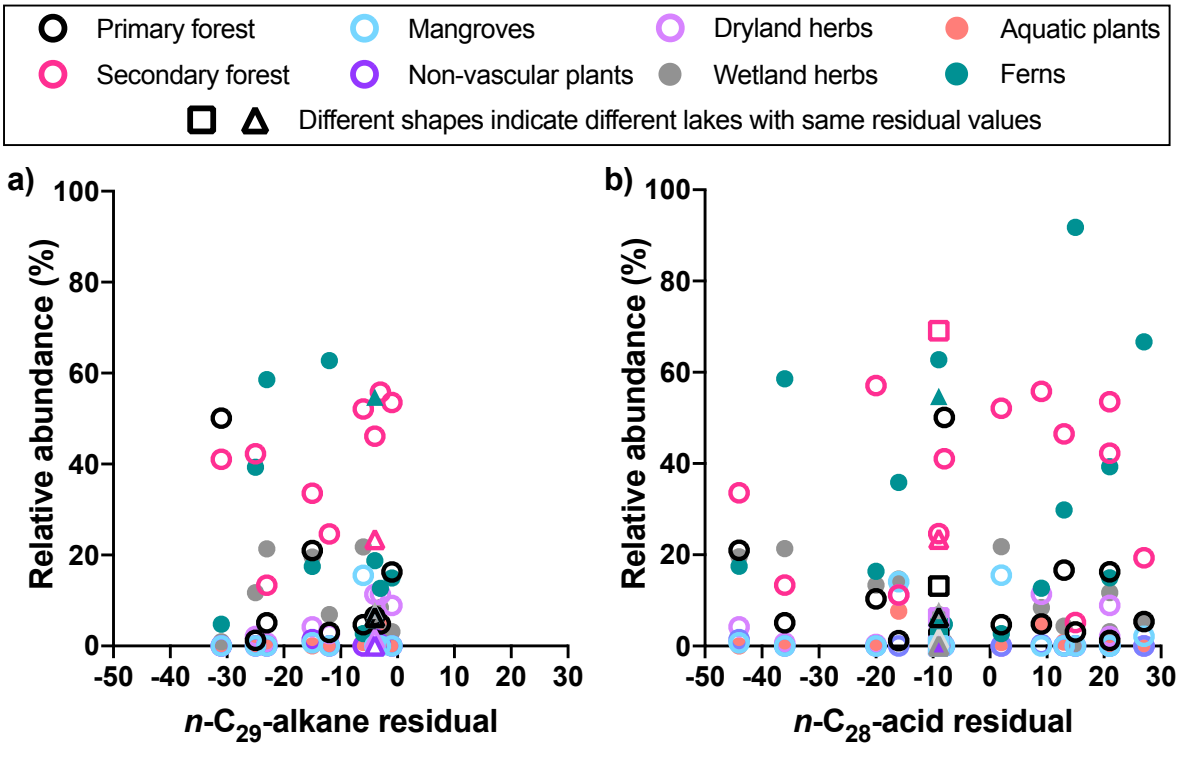
Primary forest
Secondary forest
Mangroves
Non-vascular plants
Dryland herbs
Wetland herbs
Aquatic plants
Ferns
Different shapes indicate different lakes with same residual values
a)
b)
Relative abundance (%)
0
20
40
60
80
100
-50
-40
-30
-20
-10
0
10
20
30
n-C29-alkane residual
n-C28-acid residual